



UNIVERSIDADE FEDERAL DE SERGIPE  
PRÓ-REITORIA DE PÓS-GRADUAÇÃO E PESQUISA

**ASPECTOS PETROGRÁFICOS E GEOQUÍMICOS  
DE CÔNDRULOS EM METEORITOS PRIMITIVOS:  
UM ESTUDO DE CASO A PARTIR DO METEORITO  
CAMPO SALES**

Cristine de Almeida Pereira

Orientador: Dr. Herbet Conceição

Coorientadora: Dra. Débora Correia Rios

**DISSERTAÇÃO DE MESTRADO**

Programa de Pós-Graduação em Geociências e Análise de Bacias

São Cristóvão-SE  
2023

Cristine de Almeida Pereira

**ASPECTOS PETROGRÁFICOS E GEOQUÍMICOS  
DE CÔNDRULOS EM METEORITOS PRIMITIVOS:  
UM ESTUDO DE CASO A PARTIR DO METEORITO  
CAMPO SALES**

Dissertação apresentada ao Programa de Pós-Graduação em Geociências e Análise de Bacias da Universidade Federal de Sergipe, como requisito para obtenção do título de Mestre em Geociências.

**Orientador:** Dr. Herbet Conceição

**Coorientadora:** Dra. Débora Correia Rios

São Cristóvão–SE  
2023

**FICHA CATALOGRÁFICA ELABORADA PELA BIBLIOTECA CENTRAL  
UNIVERSIDADE FEDERAL DE SERGIPE**

P436a Pereira, Cristine de Almeida  
Aspectos petrográficos e geoquímicos de côndrulos em meteoritos primitivos : um estudo de caso a partir do meteorito Campos Sales / Cristine de Almeida Pereira ; orientador Herbet Conceição – São Cristóvão, SE, 2023.  
82 f. : il.

Dissertação (mestrado em Geociências e Análise de Bacias) – Universidade Federal de Sergipe, 2023.

1. Geociências. 2. Meteoritos - Ceará. 3. Rochas - Análise. 4. Petrologia. I. Conceição, Herbet, orient. II. Título.

CDU 552.56

**ASPECTOS PETROGRÁFICOS E GEOQUÍMICOS DE  
CÔNDRULOS EM METEORITOS PRIMITIVOS: UM  
ESTUDO DE CASO A PARTIR DO METEORITO  
CAMPO SALES**

por:

Cristine de Almeida Pereira  
(Geóloga, Universidade Federal da Bahia – 2019)

**DISSERTAÇÃO DE MESTRADO**

Submetida em satisfação parcial dos requisitos ao grau de:

**MESTRE EM GEOCIÊNCIAS**

**BANCA EXAMINADORA:**

Dr. Herbet Conceição (Orientador – PGAB/UFS)

Dr. Gaston Eduardo Enrich Rojas (Membro Externo – USP)

Dra. Maria de Lourdes da Silva Rosa (Membro Interno – PGAB/UFS)

Data Defesa: 30/08/2023

*Para a menininha de 10 anos que sonhava em ser cientista.*

## AGRADECIMENTOS

Sou extremamente grata à Deus por caminhar comigo em todos os momentos de minha vida, permitindo-me vivenciar situações inesperadamente enriquecedoras. Nossa caminhada passou por momentos de vales sombrios, mas em momento algum eu me senti sozinha e desamparada.

Agradeço ao Dr. Herbet Conceição, orientador deste trabalho, por ter aceitado o desafio de “sair” de sua zona de conforto analisando uma amostra tão diferente das “comuns”. Suas palavras de desafio e reflexões sobre o assunto me inspiraram e me ajudaram a ver novos horizontes.

Agradeço à Dra. Débora Correia Rios por todos os anos de trabalho conjunto e por me apresentar ao mundo da meteorítica. Seus conselhos, dúvidas tiradas, reuniões e convivência ao longo desses 10 anos me ajudaram a acreditar no meu sonho de criança, sabendo que é possível ser uma cientista.

Não posso deixar de agradecer aos meus dois pilares de vida, minha mãe (Julie) e minha irmã (Francine). Vocês literalmente me acompanharam por todos os meus anos de vida e embarcaram das minhas ideias mais simples até as mais assustadoras. Se eu consegui chegar até onde eu estou hoje é por todo o amor e suporte que vocês me deram, nunca desacreditando dos meus sonhos e me fazendo encarar a vida com mais risadas e menos angústias.

Agradeço as minhas amigas Carmen e Ayana. Vocês foram incríveis me suportando nos momentos de crise mental e me fazendo rir das situações “inusitadas” da vida. Muito obrigada por todo o suporte e momentos ouvindo minhas lamentações.

Não posso deixar de agradecer a minha psicóloga Jucimara Neves, seu trabalho me salvou de muitos momentos de bloqueio mental e vem me ensinando a ser uma adulta que sabe de suas capacidades intelectuais e emocionais.

Agradeço a todos os colegas do programa de mestrado, pois vocês me ensinaram muito mais do que pensam. Um agradecimento especial à Victor por sua capacidade de ver o lado positivo mesmo nos momentos mais adversos. As risadas e desesperos que compartilhamos ficarão para sempre na minha memória e no meu coração.

Um especial agradecimento ao PGAB e ao LAPA por me acolherem tão bem, mesmo durante um período tão complicado de pandemia. Agradeço também à UFS e todos os órgãos de financiamento de pesquisa (CAPES, CNPq) por proporcionar a possibilidade de realizar o meu sonho de fazer um curso de mestrado.

Agradeço a Professora Maria Elizabeth Zucolotto por sua prestatividade e infinito amor pelos meteoritos da coleção brasileira.

Agradeço imensamente ao Dr. Wilton Carvalho por sua solicitude em fornecer uma amostra tão linda como a do meteorito Campo Sales, bem como à CPRM-BA por emprestar essa amostra para a pesquisa.

A todos que me apoiaram direta e indiretamente nessa caminhada, muito obrigada por estarem comigo. Nos vemos nas próximas etapas.

## **RESUMO**

Os meteoritos condrílicos representam fascinantes lembretes da história da evolução do Sistema Solar, desde o início da Nebula até a configuração vigente. Através do estudo dos côndrulos - pequenas partículas esféricas que caracterizam os meteoritos condríicos -, é possível conhecer a composição e os possíveis processos que predominavam nos primeiros estágios nebulares. Com base nisso, este estudo se propôs a ampliar a compreensão desses processos, mediante a observação dos côndrulos presentes no meteorito Campos Sales, um condrito ordinário. Este espécime apresenta côndrulos com dimensões máximas de 1 mm, cuja mineralogia é predominantemente: olivina ( $\text{Fo}_{75}$ ,  $\text{Fa}_{25}$ ), enstatita ( $\text{En}_{77}$ ,  $\text{Fs}_{23}$ ), augita ( $\text{En}_{51}$ ,  $\text{Fs}_8$ ,  $\text{Wo}_{41}$ ), e plagioclásio. Como inclusões nos côndrulos são encontrados cristais de troilita, cromita, cloroapatita e liga metálica (Fe-Ni). Em termos texturais, os côndrulos foram classificados três tipos: barrado, radial e granular. Os do tipo barrado e radial são formados, respectivamente, por cristais esqueléticos de olivina ou enstatita, com diâmetro de ~0,8 mm. Verifica-se que a associação do plagioclásio com a augita é recorrente em todos os tipos de côndrulos, formando texturas de intercrescimento. Associados ao plagioclásio também podem ser vistos cristais euédricos de cromita, enstatita e olivina. Mediante a obtenção de dados químicos dos minerais foi possível classificar o plagioclásio como oligoclásio ( $\text{Or}_6$ ,  $\text{Ab}_{84}$ ,  $\text{An}_{10}$ ), bem como constatar que muitos cristais de olivina e piroxênios têm pouca variação composicional centro-borda e estavam bem próximo ao equilíbrio com o líquido durante suas cristalizações. Sobre os processos que deram origem aos côndrulos é possível inferir que os diferentes tipos texturais foram originados, possivelmente, a partir de fontes distintas. O processo posterior de acresção destas partículas resultou na formação do corpo parental, onde os côndrulos – de natureza distintas foram - conectados pela matriz. A matriz do meteorito Campos Sales caracteriza-se principalmente pela presença de cristais subédricos de enstatita, além de cristais da liga metálica, sulfeto, merrillita, cromita, olivina e plagioclásio. A pouca variação composicional centro-borda dentro dos principais minerais que compõem os côndrulos, associada à ausência de vidro na matriz, sugerem a existência de um evento termal que devitrificou o vidro da matriz e permitiu esse reequilíbrio químico dentro dos côndrulos.

**PALAVRAS-CHAVE:** Condritos ordinários, texturas meteoríticas, processos nebulares.

## **ABSTRACT**

Chondritic meteorites represent fascinating reminders of the early history of the Solar System evolution, from the beginning of the Nebula to its current configuration. Through the study of the chondrules - small particles present in the chondrite - it is possible to learn how the composition and evolutionary processes that predominated in the first stages of nebular development. This study aimed to better understand these processes, through the mineral chemistry and petrography of the chondrules present in the Campos Sales meteorite. This meteorite shows small chondrules, with maximum dimensions of 1 mm, and a mineralogy predominantly constituted by: olivine ( $\text{Fa}_{25}$ ), enstatite ( $\text{En}_{77}$ ,  $\text{Fs}_{23}$ ), augite ( $\text{En}_{51}$ ,  $\text{Fs}_8$ ,  $\text{Wo}_{41}$ ), and plagioclase. Troilite, Fe-Ni metal alloy, chromite and chlorapatite crystals occur as inclusions. In textural terms, three types were classified: barred, radial and granular. The barred and radial chondrules display skeletal crystals of olivine or enstatite, respectively, and diameters of approximately ~0.8. It is verified that the association of plagioclase with augite is recurrent in all types of chondrules, with textures that are like intergrowth. Crystals of chromite, enstatite, and olivine were found in close association with the chondrules of plagioclase. The mineral chemistry allowed to classify this plagioclase as oligoclase ( $\text{Or}_6$ ,  $\text{Ab}_{84}$ ,  $\text{An}_{10}$ ), as well as to notice that most crystals of olivine and pyroxene have little core-border compositional variation and were very close to the equilibrium with the liquid during their crystallizations. The processes required to explain the origins of these chondrules evoke different sources areas in the nebula. Later, during the accretionary phase, these particles were combined to form Campos Sales meteorite's parental body and the groundmass that involves them. In view of the little compositional variation within the crystals and in the absence of glass in the matrix, we propose a thermal event, that devitrified the glass and allowed chondrules's chemical rebalancing.

**Keywords:** Ordinary Chondrites, meteoritic textures, nebular processes.

## **LISTA DE FIGURAS**

Figura 1. Mapa do Brasil e Rota do local do achado Campos Sales.....	14
Figura 2. Tipos texturais de côndrulos no meteorito Campos Sales .....	22
Figura 3. Imagens BSE de côndrulos barrados do meteorito Campos Sales.....	23
Figura 4. Imagens BSE de côndrulos radiais e granulares do MCS.....	24
Figura 5. Diagrama de Rhodes cristais de olivina do MCS.....	26
Figura 6. Diagrama de classificação dos piroxênios.....	26
Figura 7. Diagrama de Rhodes dos cristais de enstatita e augita.....	27
Figura 8. Diagrama de classificação para os dados dos feldspatos do MCS.....	27
Figura 9. Diagramas Binários .....	30
Figura 10. Diagrama binário de Na <sub>2</sub> O versus K <sub>2</sub> O.....	31
Figura 11. Esquema simplificado de classificação dos meteoritos.....	43
Figura 12. Imagens de fragmentos de condritos ordinários.....	46
Figura 13. Imagens de texturas em côndrulos obtidas na literatura.....	47

## **LISTA DE TABELAS**

Tabela 1. Comparação entre as composições de padrões internacionais e os dados obtidos com EDS-MEV neste estudo.....	20
Tabela 2. Variação das composições químicas dos minerais presentes nos côndrulos estudados do meteorito Campos Sales.....	25
Tabela 3. Variação dos óxidos no centro e na borda em cristais de olivina, enstatita e augita.....	25
Tabela 4. Composição química dos côndrulos do MCS .....	28
Tabela 5. Composição química dos côndrulos do MCS.....	28
Tabela 6. Dados de composição química para côndrulos de Olivina Granular (GO).....	29
Tabela 7. Dados de composição química para côndrulos de Olivina Barrada (BO).....	29
Tabela 8. Dados de composição química para côndrulos de Olivina Piroxênio Granular.....	29
Tabela 9. Classificação dos Côndrulos.....	48

## SUMÁRIO

Capítulo I: Introdução.....	13
Referências .....	16
Capítulo II: <b>Unraveling the Origins of the Solar System: A Comprehensive Petrological Investigation of Chondrules within the Campos Sales Meteorite.....</b>	<b>17</b>
<i>Introdução.....</i>	<i>18</i>
<i>Materiais e Métodos.....</i>	<i>19</i>
<i>Resultados.....</i>	<i>20</i>
<i>Discussões.....</i>	<i>31</i>
<i>Conclusões.....</i>	<i>34</i>
<i>Referências.....</i>	<i>36</i>
Capítulo III: Conclusões.....	39
Anexos.....	43
<i>Estado da Arte.....</i>	<i>43</i>
<i>Normas para Publicação.....</i>	<i>52</i>
<i>Tabelas de dados.....</i>	<i>66</i>

## **CAPÍTULO I: INTRODUÇÃO**

## I. INTRODUÇÃO

O meteorito Campos Sales (MCS), objeto de estudo deste trabalho, é um corpo cuja queda foi presenciada em 31 de janeiro de 1991, na área rural da cidade de Campos Sales, Ceará, Brazil. Os fragmentos de rocha coletados totalizaram em uma massa de aproximadamente 23 kg, e o meteorito foi classificado como um condrito ordinário L5 com baixo índice de choque (Scorzelli *et al.*, 1998).

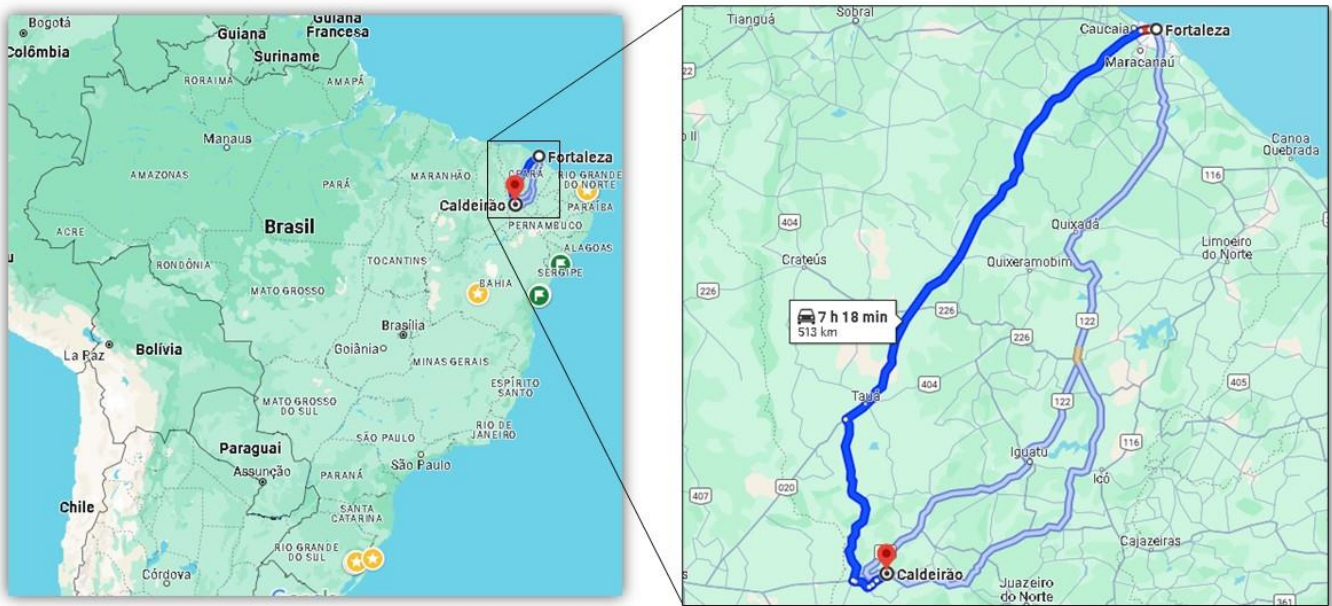


Figura1. Mapa do Brasil (a esquerda) e Rota do local do achado Campos Sales/ Caldeirão até Fortaleza- Ceará (a direita). Fonte: Google Maps.

Apesar de ser conhecida a localização de queda do MCS, não se conhece com precisão seu corpo originário. Segundo estudos de Meier et al. (2017) e de Jenniskens et al. (2019), condritos do tipo L são associados com corpos parentais asteroidais presentes no cinturão de asteroides de Júpiter. No caso específico dos condritos L5, associa-se a origem dessas rochas com a fragmentação de asteroides da família Gefion, cuja quebra do corpo original ocorreu a  $4497 \pm 6$  Ma atrás segundo idades obtidas pelos métodos de U-Pb e Pb-Pb(Jenniskens et al., 2019).

Mediante a essas informações, o presente estudo, visou a obtenção de dados petrográficos e mineraloquímicos dos côndrulos presentes na amostra do MCS disponível, a fim de estudar os côndrulos e os minerais que compõem a rocha de maneira mais detalhada.

As informações e conclusões obtidas pretendem ser publicadas na revista *Meteoritics and Planetary Science*, que atua como um dos principais expoentes na divulgação de informações da área meteorítica.

## Referências

- Jenniskens, P., Utas, J., Yin, Q., Matson, R.D., Fries, M., Howell, J. A., Free, D., Albers, J., Devillepoix, H., Bland, P., Miller, A., Verish, R., Garvie, L.A.J., Zolensky, M.E., Ziegler, K., Sanborn, M.E., Verosub, K.L., Rowland, D.J., Ostrowski, D.R., Bryson, K., Laubenstein , M., Zhou, Q., Li Q.L., Li, X.H., Liu, Y., Tang, G.Q., Welten, K., Caffee, M.W., Meier, M.M.M., Plant, A.A., Maden, C., Busemann, H., Granvik, M. 2019. The Creston, California, meteorite fall and the origin of L chondrites. *Meteoritics & Planetary Science*. 54, 699–720. doi: 10.1111/maps.13235
- Meier. M.M.M., Welten, K.C., Riebe, M.E.I., Caffee, M.W., Gritsevich, M., Maden, C., Busemann, H. 2017. Park Forest (L5) and the asteroidal source of shocked L chondrites. *Meteoritics & Planetary Science*. 52, 1561-1576. doi: 10.1111/maps.12874
- Scorzelli, R.B., Christophe Michel-Lévy, M., Gilabert, E., Lavielle, B., Souza Azevedo, I., Vieira, V.W., Costa, T.V.V., Araújo, M.A.B. 1998. The Campos Sales meteorite from Brazil: a lightly shocked L5 chondrite fall. *Meteoritics and Planetary Science*. 33, 1335-1337. doi.org/10.1111/j.1945-5100.1998.tb01317.x

**CAPÍTULO II: Unraveling the Origins of the Solar System: A Comprehensive Petrological Investigation of Chondrules within the Campos Sales Meteorite**

**Unraveling the Origins of the Solar System:  
A Comprehensive Petrological Investigation of Chondrules within the Campos Sales Meteorite**

Cristine de Almeida Pereira\*<sup>1,2</sup>, Herbet Conceição<sup>1</sup>, Débora Correia Rios<sup>2,3</sup>

<sup>1</sup> Universidade Federal de Sergipe. Instituto de Geociências. Programa de Pós-Graduação em Geociências e Análises de Bacias, Complexo Laboratorial Multiusuário. Avenida Marechal Rondon, s/n, Jardim Rosa Elze, São Cristóvão. 49.100-000, Aracaju, Sergipe – Brasil. E-mails: [cristinepereira1@gmail.com](mailto:cristinepereira1@gmail.com), [herbet@academico.ufs.br](mailto:herbet@academico.ufs.br)

<sup>2</sup> Universidade Federal da Bahia. Instituto de Geociências. Geologar – Ciências da Terra para a Sociedade, Laboratório de Petrologia Aplicada a Pesquisa Mineral. Programa de Pós-Graduação em Geologia. Rua Barão de Jeremoabo, s/n, Campus Universitário de Ondina. 40.170-290, Salvador, Bahia – Brasil. E-mail: [drios2016@gmail.com](mailto:drios2016@gmail.com)

<sup>3</sup> Western Ontario University, Zircon and Accessory Phases Laboratory – ZAPLab, Department of Earth Sciences, University of Western Ontario. 1151, Richmond St. N., London, Ontario, N6A 5B7, Canada.

\* Corresponding author

## ABSTRACT

This paper investigates chondrules, integral components of chondritic meteorites from the early Solar System. Focusing on 33 chondrules from the Campos Sales Meteorite, an L5 ordinary chondrite, we explore their compositions, mineral formation, and origin. Considering the hypothesis that chondrules may be "magmatic" droplets, we examine the compositions of these "primitive melts." Campo Sales' chondrules, mostly circular with some undefined shapes, contain olivine, enstatite, augite, chromite, troilite, Cl-apatite, and silicon dioxide. Varied textures, including barred, radial, and granular patterns, alongside skeletal crystals of olivine, enstatite, and augite, are observed, some featuring intergrowth textures. Chemical data reveal compositional homogeneity, indicating a chemical reequilibration event. Despite challenges in discerning elemental patterns, the study underscores rapid crystallization and preservation of skeletal shapes and volatile elements, suggesting accretion before complete solidification. These findings offer insights into early Solar System evolution, emphasizing chondrules as records of magmatic processes amid challenges in understanding their elemental patterns. The study provides comprehensive insights into type L chondrules, unraveling their composition, formation, and the intricate processes shaping the early Solar System.

## Keywords:

Chondrules,  
Campo Sales Meteorite,  
Petrography,  
Geochemical Compositions,  
Solar System Formation,  
Origins Processes.

## HIGHLIGHTS

1. The petrological aspects of Campo Sales meteorite sheds light on the enigmatic evolution of the early Solar System, providing glimpses into its formative processes.
2. Chondrules are key observatories providing valuable insights into the early Solar System's evolution. Chondrules within the Campos Sales Meteorite serve as critical windows into formative processes, sparking debates over planetary or nebular origins.
3. The diversity of chondrules within the Campo Sales meteorite contribute to unique mineralogical signatures. Petrographic scrutiny unveils irregular fractures, adding complexity to mineral composition. Classification identifies three main chondrule groups – barred olivine, radial enstatite, and granular – each characterized by distinctive characteristics.
4. L-type chondrules, despite exhibiting a spherical tendency, exhibit pronounced deformation, challenging assumptions of uniform pressure. This suggests dynamic interactions and resilience within dynamic environments.
5. Chemical data indicate minimal compositional variability within “balanced” chondrites. The prevalence of skeletal olivine and pyroxenes suggests rapid crystallization from magnesium and iron-rich materials during distinct magmatic events, offering insights into the chondrite’s geological history.
6. The “balanced” nature of some chondrites give valuable insights into the processes and conditions present in the early solar system. Deformation and agglutination dynamics provide clues to non-simultaneous crystallization, highlighting distinct occurrences during the early Solar System.
7. This investigation unravels complexities in type L chondrules, challenging existing paradigms. Chondrules emerge as records of magmatic processes, inviting a reevaluation of our understanding amid ongoing challenges in deciphering their elemental patterns.

## INTRODUCTION

Meteorites, remnants of extraterrestrial rocks penetrating Earth's atmosphere, primarily originate from asteroids and, to a lesser extent, Mars, the Moon, and comets (Rubin & Ma, 2020). Beyond their captivating luminous displays, meteorites have intrigued humanity for millennia, as evidenced by historical accounts such as the Egyptians using "metal from the sky" in artifacts like King Tutankhamun's dagger (Comelli et al., 2016, Wang & Korotev, 2019). Classified based on petrographic characteristics and geochemical compositions, meteorites encompass various groups, reflecting distinct formation processes like condensation around newly formed stars, crystallization from chondritic melts, aqueous alterations, and shock metamorphism (Rubin & Ma, 2020).

Among meteorites, chondrites, which are rich in chondrules, provide crucial insights into the early Solar System (Scott & Krot, 2005). These meteorites originated from the fusion and consolidation of their parent bodies, sparking increased study in the 19<sup>th</sup> century and subsequent debates on planetary versus nebular processes. In 1864, H. C. Sorby proposed a groundbreaking idea, suggesting that chondrites' material might have originated from fusion, subsequent fragmentation, and consolidation due to the mechanical and chemical actions of their parent body (Merrill, 1920). However, it wasn't until the 1960s that investigations took a more profound turn.

During this pivotal period, two prevailing perspectives emerged on the origin of chondrules: (i) formation through planetary processes proposed by Urey in 1954, or (ii) formation through nebular processes as suggested by Wood in 1963 and Larimer & Anders in 1967. By the 1970s, studies confirmed chondrites' nebular origin (Grossman and Larimer, 1974).

The current classification of chondrules considers their mineralogical-textural characteristics and FeO content, resulting in two primary groups: type I, characterized by low FeO (<10% wt.), and type II, with high FeO (>10% wt.). Subcategories within these groups are further defined based on the prevalence of olivine (A) or pyroxene (B), as well as observed textures such as barred, radial, granular, porphyritic, microcrystalline, among others (Gooding & Keil, 1981). Regarding shape, the prevailing notion, rooted in the belief that chondrules originate from solidified droplets, asserts that these particles should ideally exhibit a spherical form. However, in reality, chondrules manifest in both spherical and non-spherical forms, including fragments of spheres or shapes resembling droplets (Hewins, 1997).

The processes governing chondrule formation remain incompletely understood. Some researchers propose that these particles underwent at least one melting event before being incorporated into the parent body (Desch et al., 2012; Johnson et al., 2015; Morris et al., 2016). Additionally, the enigmatic formation of chondrules involves not only melting events but also rapid cooling, leading to the development of skeletal crystals composed of olivine and pyroxenes (Hewins, 1997).

Expanding on our existing understanding of meteorite textures and mineralogy, and operating under the assumption that chondrules serve as the primary droplets of magmas in the Solar System, a fundamental inquiry arises: What constitutes the composition of the material that gave rise to these chondrules? Does a singular material underlie diverse chondrules through distinct formation processes, or do different sources contribute to their origins? To address these questions comprehensively, we conducted an extensive assessment of the petrography and mineral chemistry of submillimeter chondrules from the Campos Sales meteorite. The fall of the Campos Sales meteorite (MCS) was witnessed on January 31, 1991, in the town of Campos Sales, Ceará, Brazil (Scorzelli et al., 1998). Weighting 23.68 kg, the recovery mass of this meteorite was subsequently classified as an ordinary chondrite of the L5 type.

## MATERIALS AND METHODS

In this investigation, we employed a polished thin section obtained from a fragment of the Campos Sales meteorite, generously provided by Dr. Wilton Carvalho. The total analyzed area of this thin section approximates 8 cm<sup>2</sup>. Our examinations utilized both petrographic and scanning electron microscopes (SEM) at the Condomínio de Laboratórios Multiusuários das Geociências of the Universidade Federal de Sergipe, Brazil.

The SEM, a Tescan Veja 3 LMU model, was equipped with detectors for secondary electrons, backscattered electrons (BSE), cathodoluminescence, and energy dispersive spectroscopy (EDS). The thin section underwent an initial gold coating (8-10 nm thickness), followed by cleaning and carbon coating to enhance observations in the petrographic microscope.

### Microanalysis:

The SEM, utilizing the backscattered electron (BSE) detector for texture analysis, captured images of the sample. Chemical compositions of the minerals were acquired using EDS (Oxford Instrument X-Act model) with a resolution of 125 eV. Internal calibration of the EDS involved standards with precise measurements ( $2\sigma$ ), including albite albite (NaK $\alpha$ ,  $\pm 0.2$ ), corundum (AlK $\alpha$ ,  $\pm 0.2$ ), metallic chromium (CrK $\alpha$ ,  $\pm 0.4$ ), fluorite (FK $\alpha$ ,  $\pm 0.3$ ), metallic iron (FeK $\alpha$ ,  $\pm 0.4$ ), halite (ClK $\alpha$ ,  $\pm 0.3$ ), metallic manganese (MnK $\alpha$ ,  $\pm 0.2$ ), metallic nickel (NiK $\alpha$ ,  $\pm 0.3$ ), orthoclase (KK $\alpha$ ,  $\pm 0.2$ ), periclase (MgK $\alpha$ ,  $\pm 0.4$ ), quartz (SiK $\alpha$ ,  $\pm 0.4$ ), metallic titanium (TiK $\alpha$ ,  $\pm 0.2$ ), wollastonite (CaK $\alpha$ ,  $\pm 0.2$ ).

The analytical conditions for EDS-SEM were set at 20 kV voltage, 17 nA intensity, 0.4  $\mu$ m electron beam diameter, 60-240 s (average counting time), and 15 mm analysis distance. Analytical data were processed using AztecEnergy software (version 4.0, Oxford Instruments®), employing ZAF corrections for “Quant routine” analysis and accurate oxide percentage calculations. Rigorous correction procedures for false peaks, escape peaks, and coincident energy peaks were applied following Newbury's recommendations (2009). To ensure accuracy and reliability, the results underwent verification against mineral standards and oxides from Astimex Scientific Ltd®, Cameca, and internal standards of CLGeo (**Table 1**).

**Table 1:** Comparison between the compositions of international standards (AST, CAM) and the data acquired through Energy Dispersive Spectroscopy – Scanning Electron Microscope (EDS-SEM) in the current study. The abbreviations used are AST (Astimex standards), EM for EDS-SEM, CAM (Cameca Standards). The column labeled “ $2\Theta$ ” denotes the difference between the standards and the EDS-SEM data, providing a quantitative measure of the variance between the two datasets.

	Olivine			Cr-Diopside			Fosterite			Fayalite			Enstatite			Diopside			Cl-Apatite			Phosphate					
	AST	EM	2Θ	AST	EM	2Θ	CAM	EM	2Θ	CAM	EM	2Θ	CAM	EM	2Θ	CAM	EM	2Θ	CAM	EM	2Θ	CAM	EM	2Θ			
SiO <sub>2</sub>	41.85	41.08	0.26	55.13	55.43	0.27	43.63	43.94	0.27	29.48	29.75	0.24	59.85	59.21	0.31	55.49	55.89	0.27									
TiO <sub>2</sub>				0.05	0.09	0.08																					
FeO	6.51	6.68	0.14	1.21	1.21	0.10				70.52	70.25	0.25															
MgO	51.57	51.81	0.24	17.46	18.14	0.17	56.34	56.06	0.23				40.15	40.36	0.22	18.62	18.58	0.17									
MnO	0.12	0.12	0.07																								
CaO				25.55	24.60	0.16										25.90	25.54	0.16	53.30	53.83	0.21	43.94	44.79	0.20			
NiO	0.20	0.32	0.09																								
Cr <sub>2</sub> O <sub>3</sub>				0.58	0.53	0.08																39.90	39.45	0.28	53.98	54.06	0.30
P <sub>2</sub> O <sub>5</sub>																						6.80	6.73	0.09			
Cl																									1.21	1.16	0.11
V <sub>2</sub> O <sub>5</sub>																											
Total	100.30	100.00		99.98	100.00		100.00	100.00		100.00	100.00		100.00	99.57		100.00	100.00		100.00	100.00		99.13	100.00				

## Analysis and Classification:

Chemical analyses covered crystals of minerals within chondrules and the matrix. Structural formulas were computed for pyroxenes, olivine, and plagioclase, with analyses falling within an acceptable range of variation. The area calculation tool available in the AztecEnergy software was used. The 33 well-defined chondrules underwent total composition studies and correlation of composition versus area. Manual delimitation marked the boundaries of each chondrule, guided by texture observation, imaging, and chemical data, leading to their textural classification into three distinct groups: barred, radial, and granular.

Chemical data treatment employed GCDKit® software for graph generation, observing chemical correlations and affinities. Additionally, the MagMin\_PT® program (Gündüz and Asan, 2022) calculated crystallization pressures and temperatures using algorithms from various authors. Abbreviations for mineral names followed IMA-CNMNC approved mineral symbols (Warr, 2021).

## RESULTS

### Chondrule Diversity and Petrographic Insights:

The examination of the Campos Sales meteorite (MCS) provides a nuanced understanding of chondrule diversity and petrographic features. In this 8.14 cm<sup>2</sup> polished thin section, chondrules, ranging from millimeter to submillimeter sizes, compose a significant portion (~40%) of the specimen. They are subtle to the naked eye yet distinctly preserved in thin sections. Three distinct components emerge: well-defined chondrules, fragments with relic structures, and a crystalline matrix, contributing to a holistic petrographic landscape.

MCS unveils a rich mineralogy, including olivine (Fo<sub>74-78</sub>), orthopyroxene (En<sub>75-79</sub>, Fs<sub>25-21</sub>), clinopyroxene (En<sub>47-54</sub>, Fs<sub>8</sub>, Wo<sub>45-58</sub>), chromite (Sp<sub>15</sub>, Mt<sub>2</sub>, Usp<sub>6</sub>, Chr<sub>77</sub>), kamacite (90% < Fe < 93% and 5% < %Ni < 7%), taenite (79% < Fe < 87% and 11% < Ni < 18%), tetrataenite (68% < Fe < 40% and 27% < Ni < 55%), Cl-apatite (4% < Cl < 6%), troilite (32% < S < 40% and 54% < Fe < 65%), merrillite (Ca<sub>18</sub>Na<sub>2</sub>Mg<sub>2</sub>(PO<sub>4</sub>)<sub>14</sub>), plagioclase (Or<sub>6</sub>, Ab<sub>84</sub>, An<sub>10</sub>), silicon dioxide, and ilmenite. Noteworthy is the presence of irregular fractures, particularly visible in olivine and pyroxene crystals, while no shock veins are observed, and adding a layer of complexity to the mineral composition of this meteorite.

### Chondrule Characterization and Classification:

Chondrules within MCS exhibit diverse characteristics, with calculated diameters ranging from 0.8 mm to 2 mm and areas varying across a spectrum (from 0.078 mm<sup>2</sup> to 3.413 mm<sup>2</sup>). No distinct predominance in diameter or area is noted among different chondrules. Olivine, enstatite, augite, and oligoclase emerge as primary constituents of chondrules, accompanied by accessory minerals including troilite, Fe-Ni alloy, chromite, Cl-apatite, and silicon dioxide. A meticulous classification yields three main chondrule groups,

based on main mineral content (>80% olivine or pyroxene) and textural aspects: barred olivine, radial enstatite, and granular (**Figures 1, 2, 3**), each contributing distinctive mineralogical signatures.

#### *Barred Chondrules: A Microscopic Mosaic of Olivine Dominance*

Within the barred chondrules, depicted vividly in **Figures 1A and 2**, a captivating interplay of minerals unfolds. The dominant presence of skeletal olivine crystals, boasting a %Fo exceeding 80%, characterizes these chondrules. These crystals, ranging from fractured to intact, exhibit a parallel orientation and lengths of up to 1 mm. The interstices between the olivine crystals host a diverse assembly, including pyroxene crystals (enstatite and augite), chlorapatite, plagioclase, and chromite.

In certain chondrules with a barred texture, an additional layer of complexity emerges. Anhedral olivine crystals (<30 µm) intricately associate with plagioclase (<30 µm) and pyroxenes (<40 µm). **Figures 2B and 2C** unveils the presence of euhedral chromite crystals (4-6 µm), forming an intriguing intergrown appearance with plagioclase and augite crystals. Notably, twinning in plagioclase crystals remains absent in the thin section.

The microscopic landscape extends its richness with rare occurrences of microspheres of silicon dioxide, boasting diameters of up to 2.5 µm (**Figure 2D**). These microspheres, sporadic in occurrence, find association with olivine crystals and, at times, plagioclase. As the exploration moves toward the outer zone of the barred chondrules, dispersed anhedral troilite crystals and fragments of the metallic alloy make their presence known, contributing to the intricate mosaic of mineralogical diversity.

#### *Subtle Rhythms: Exploring the Enigmatic World of Radial Texture Chondrules*

In the radial texture chondrules (**Figures 1B and 3A**), enstatite takes center stage with skeletal crystals (%En > 60%) ranging from 0.07 to 0.7 mm, exhibiting fractures devoid of preferential directions. Within this intricate structure, subhedral olivine crystals coexist with plagioclase and augite crystals (<50 µm), showcasing a texture akin to intergrowth. This phenomenon may stem from exsolution or eutectoid formation processes. The presence of fractures, lacking a distinct directionality and potentially filled with plagioclase crystals, adds to the complexity of this captivating microscopic world.

Diverging from their barred counterparts, radial chondrules boast a heightened abundance of sulfide crystals dispersed throughout their interior, allowing to explore the nuanced details of their formations as we unravel the distinctive characteristics within this radial texture.

#### *The Mosaic: Unraveling the Chondrules of Granular Texture*

The granular texture (**Figures 1C and 3C**) unfolds as distinct segments within chondrules, diverging from the mineralogical patterns observed in barred olivine or radial pyroxene textures. This textural type reveals an intriguing interplay, showcasing the coexistence of plagioclase with augite and enstatite, reminiscent of the associations observed in the other two chondrule types.

#### **Insights into Chondrule Shape and Deformation:**

Moreover, upon closer scrutiny, a consistent tendency emerges among chondrules, transcending their textural classifications, to assume a spherical morphology. Despite this prevailing spherical inclination in numerous chondrules, the visual landscape is punctuated by indications of deformation (**Figure 3C**), causing alterations in their shapes. In certain instances, this deformation is so pronounced that it results in the disintegration of the chondritic structure itself. Within this intricate pattern, glimpses into the fundamental nature of the material become discernible only when traces of residual structures endure, underscoring the impact of substantial deformation on their morphology and offering insights into the resilience of chondrules within dynamic environments.

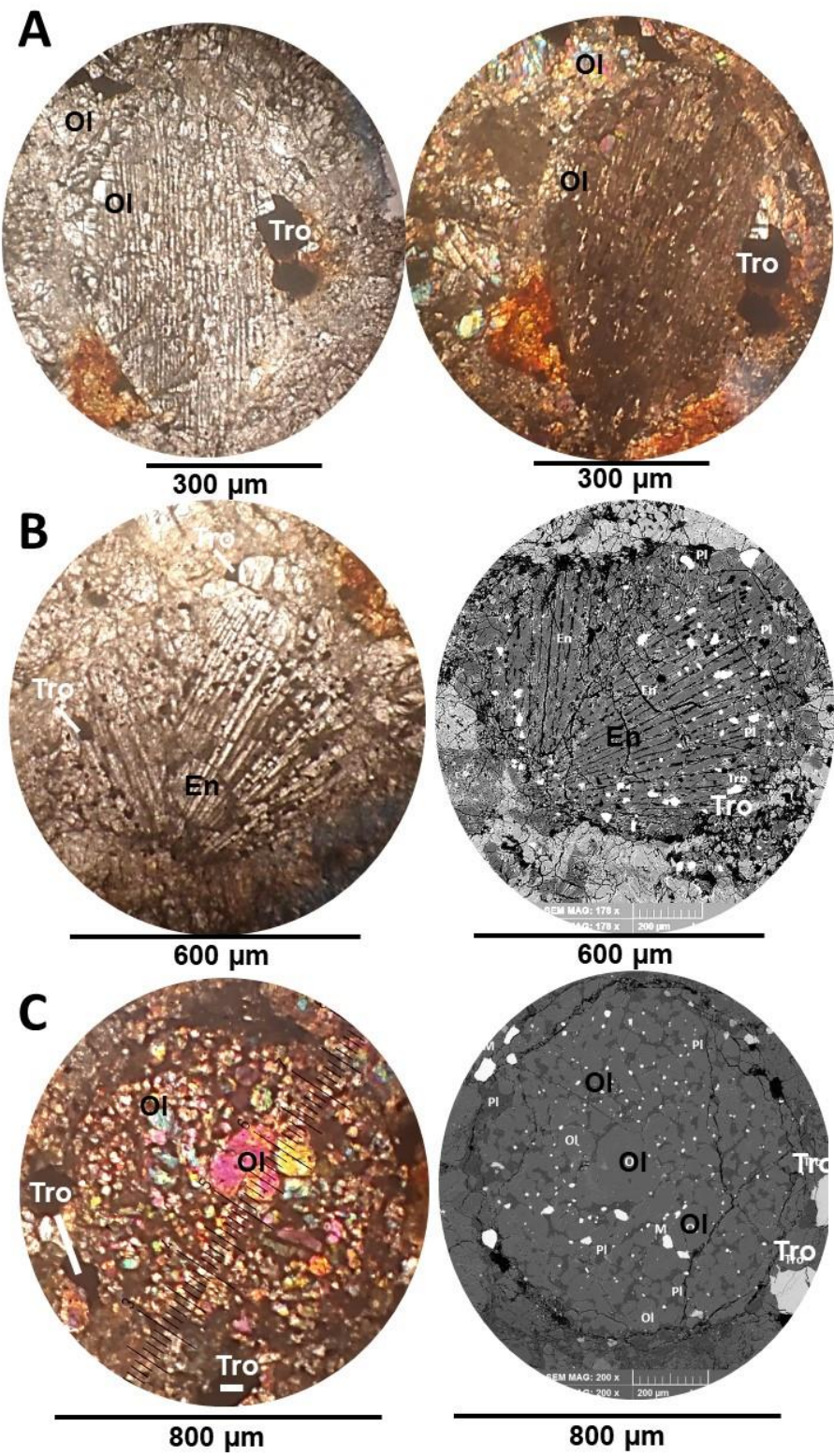


**Figure 1:** Textural Varieties of Chondrules within the Campo Sales Meteorite (MCS). Detailed visual representations using various microscopy techniques: (A) Barred Olivine: Displaying an image captured with polarized light on the left and plain light on the right. (B) Radial Pyroxene (Enstatite): Featuring a backscattered electron (BSE) image on the left and a plain light image on the right. (C) Granular: Showcasing a BSE image on the left and a polarized light image on the right.

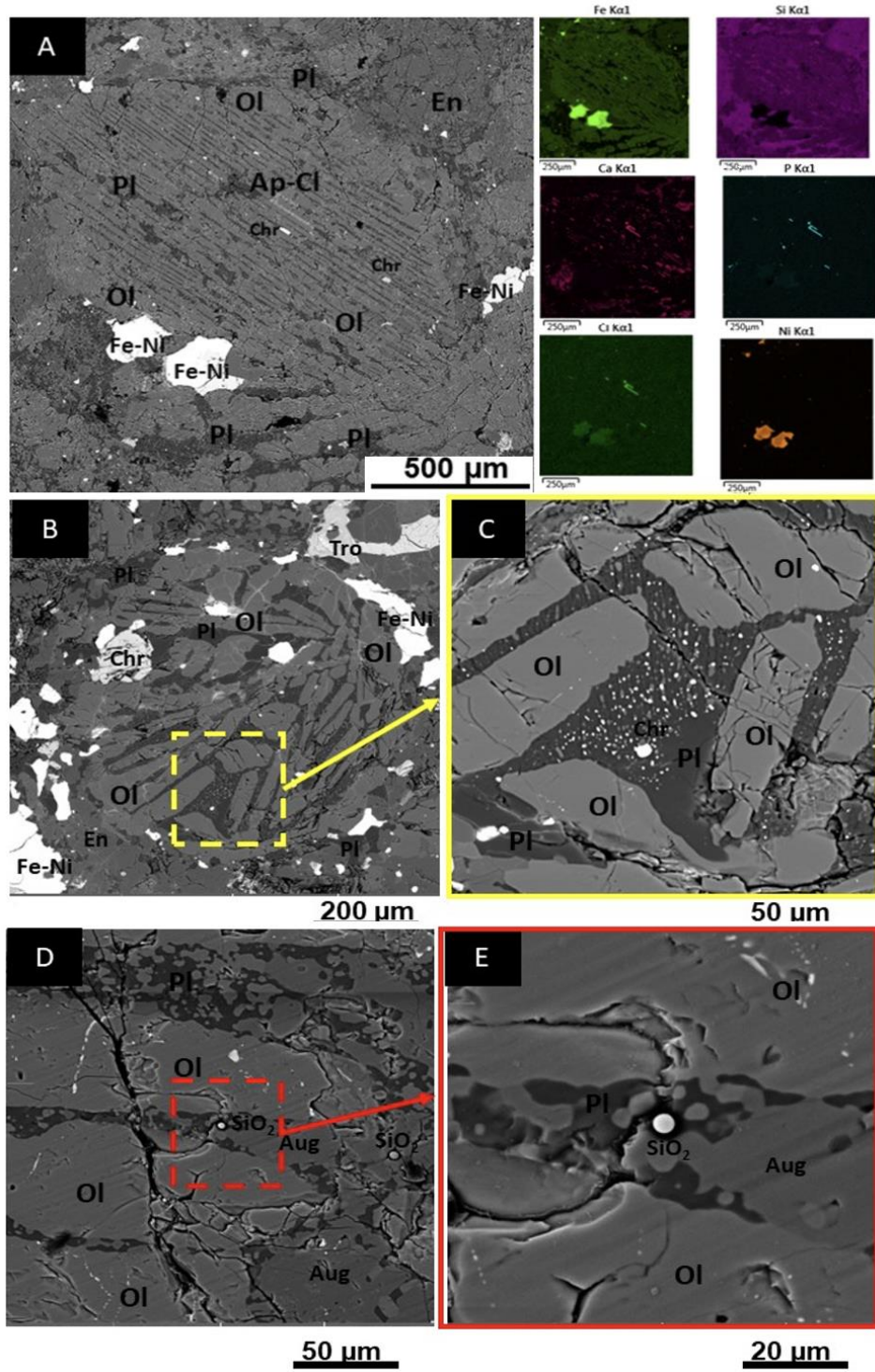


**Figure 2:** Backscattered Electron (BSE) Images, accompanied by elemental distribution maps, of Barred Chondrules in the Campos Sales Meteorite. (A) On the left, a barred olivine chondrule exhibiting skeletal olivine (Ol) crystals, plagioclase (Pl) crystals, interstitial chromite (Chr), and chlorapatite (Ap-Cl) crystal. Surrounding the chondrule are Fe-Ni and enstatite (En) crystals. On the right, false-color elemental maps depict the distribution of Fe, Si, Ca, P, Cl, and Ni. (B) Barred chondrule featuring a more randomly arranged configuration of skeletal olivine crystals. Notable are the plagioclase crystals interspersed between olivine crystals and the presence of a chromite crystal. (C) Detail of image B (bottom center - highlighted in yellow) emphasizing plagioclase and micrometer-sized chromite crystals positioned between the skeletal olivine crystals. Light gray crystals correspond to augite, and white dots represent chromite crystals. (D) Detail of a barred chondrule highlighting the presence of silicon dioxide spheres in conjunction with plagioclase and augite (Au) crystals nestled among the skeletal olivine crystals. (E) Detail of image D (highlighted in red) focusing on the area with silicon dioxide sphere presence.

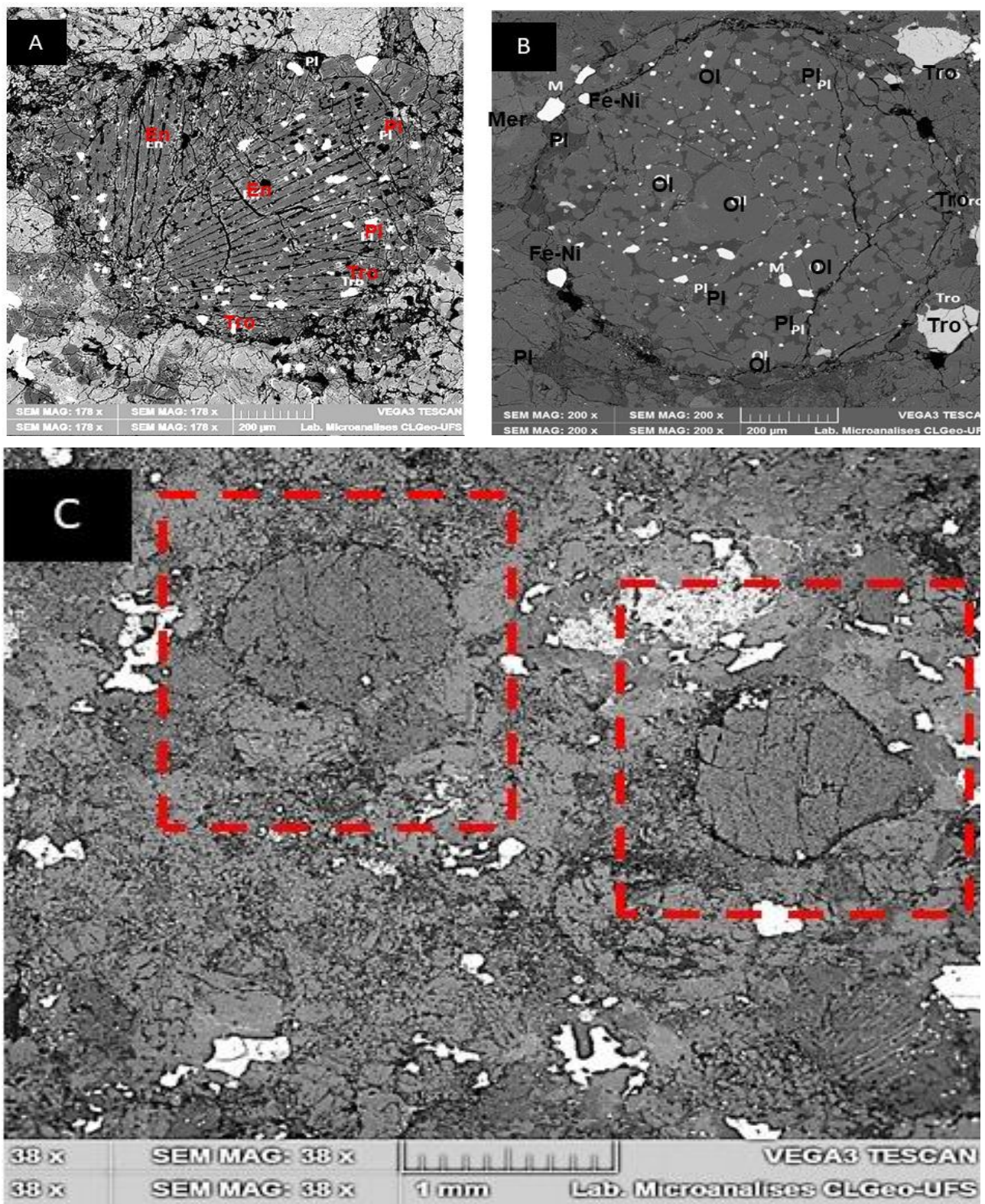


**Figure 3:** Backscattered Electron (BSE) Imaging providing insights into the structural features of radial and granular chondrules within the Campos Sales Meteorite, enhancing our understanding of their internal composition and shape variations. (A) Radial chondrule featuring skeletal enstatite (En) crystals with interstitial plagioclase (Pl) crystals. The chondrule exhibits the presence of troilite (Tro) crystals within. (B) Granular chondrule predominantly composed of olivine (Ol) and plagioclase (Pl) crystals. Peripheral zones of the crystal contain Fe-Ni and troilite crystals, while an outer portion of the chondrule displays a merrillite (Mer) crystal. (C) Chondrules presented with preserved shapes, along with one chondrule highlighted in red, showcasing a distinctly deformed shape.

## Unlocking Elemental Chronicles: Analyzing Mineral Compositions and Chondrule Equilibria

The chemical analysis focused on unraveling the intricacies of both mineral and chondrule compositions, offering a comprehensive view of the Campos Sales meteorite's elemental makeup. **Table 2** provides a detailed overview of the chemical variations within the analyzed minerals, excluding metallic alloy and sulfide. Observations reveal a consistent composition for ferromagnesian silicate crystals in both the matrix and chondrules of MCS (**Table 3**).

**Table 2:** Chemical Composition Variation of Minerals in Studied Chondrules from the Campos Sales Meteorite.

Mineral / Oxide (% wt)	Olivine		Enstatite		Augite		Chromite		Merrillite		Cl-Apatite		Plagioclase	
SiO <sub>2</sub>	37.73	40.77	55.50	56.20	52.80	54.80	0.94	4.89	0.30	2.31	0.60	2.04	61.26	66.14
TiO <sub>2</sub>		0.02	0.40	0.30	0.60	0.20	2.47	1.71	0.01	0.21	0.02	0.20	0.09	
Al <sub>2</sub> O <sub>3</sub>		1.32	0.20	0.20	3.60	0.40	2.89	6.61		13.94	0.22	0.71	17.02	21.55
Cr <sub>2</sub> O <sub>3</sub>	0.08	0.01	0.40	0.10	2.60	0.50	59.91	40.63		0.02			0.09	
FeO	22.52	19.75	12.70	11.70	5.10	5.20	30.17	41.09	0.53	1.72	0.76	11.82	4.35	0.53
MnO	0.43	0.43	0.50	0.40	0.30	0.30	0.54	0.66		0.04	0.04	0.02	0.08	
MgO	39.11	37.00	29.40	30.40	14.50	18.10	1.01	1.85	4.17	5.56	0.06	0.43	5.43	
CaO	0.06	0.46	0.80	0.80	18.50	19.70	0.07	0.15	45.98	37.34	50.50	38.60	1.78	2.51
Na <sub>2</sub> O		0.25			2.00	0.50	0.23	0.95	3.15	2.04	0.59	0.69	8.96	7.27
K <sub>2</sub> O		0.08		0.10		0.10	0.01	0.06		0.08		0.04	0.54	1.49
P <sub>2</sub> O <sub>5</sub>	0.01						0.23		45.56	36.58	40.56	30.72		
CO <sub>2</sub>												9.41		
Cl									0.08		5.12	4.15		
<b>Total</b>	<b>99.94</b>	<b>99.95</b>	<b>100.00</b>	<b>100.00</b>	<b>99.90</b>	<b>99.80</b>	<b>98.47</b>	<b>98.60</b>	<b>99.78</b>	<b>99.84</b>	<b>98.83</b>	<b>98.47</b>	<b>100.00</b>	<b>99.55</b>

**Table 3:** Variation in Chemical Compositions (%wt. = weight percent) of Olivine, Enstatite, and Augite Crystals at the Center and Edge. The data provides insights into the elemental variations within these crystals at distinct structural locations.

Mineral / Oxide (% wt)	Olivine		Enstatite		Augite	
	Center	Edge	Center	Edge	Center	Edge
SiO <sub>2</sub>	38.13	37.21	56.46	56.14	55.99	55.49
TiO <sub>2</sub>		0.20	0.24	0.10	0.37	0.37
Al <sub>2</sub> O <sub>3</sub>	0.01		0.06	0.34	0.44	0.30
FeO	22.04	23.10	11.20	11.23	3.71	4.16
MnO		0.48	0.31	0.34	0.16	0.22
MgO		38.74	30.94	30.54	18.69	17.88
CaO			0.55	0.84	19.55	20.78
Na <sub>2</sub> O			0.04	0.06	0.59	0.28
K <sub>2</sub> O			0.05			0.02
<b>Total</b>	<b>60.18</b>	<b>99.73</b>	<b>99.85</b>	<b>99.59</b>	<b>99.50</b>	<b>99.50</b>

Further examination of olivine crystals ( $n=18$ ) using the Rhodes diagram (Rhodes 1970, **Figure 4**) indicates equilibrium with the liquid during crystallization, showcasing a dynamic interplay between elements. Orthopyroxene crystals ( $n=20$ ) predominantly fall within the enstatite field, while clinopyroxene crystals ( $n=25$ ) correspond to augite, with some bordering augite and diopside (**Figure 5**). Equilibrium analysis between orthopyroxene crystals and the liquid (**Figure 6**) illustrates a distinct trend, emphasizing non-equilibrium conditions. Augite crystals, on the other hand, exhibit a closer alignment with the equilibrium line. Plagioclase crystals ( $n=28$ ) predominantly display albite composition, with some exhibiting oligoclase composition and a lone crystal at the oligoclase-andesine boundary (**Figure 7**). No clear correlation emerges between petrographic and chemical data.

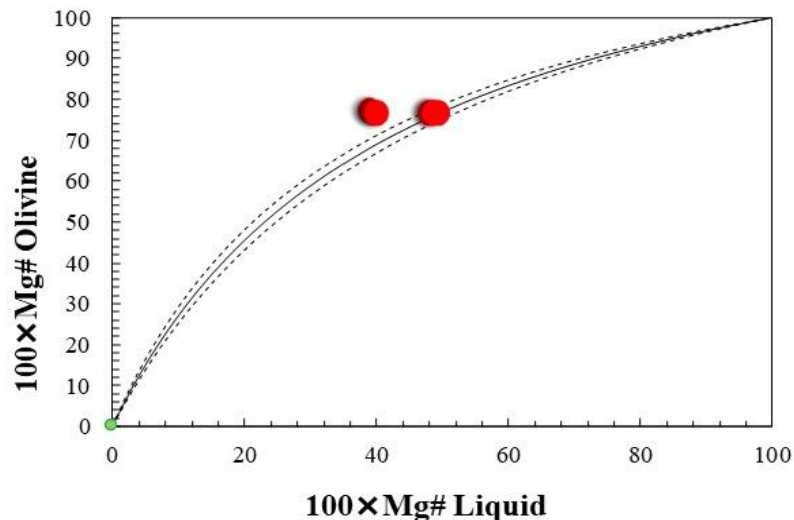


**Figure 4:** Rhodes Diagram for Assessing Equilibrium with Liquid during Olivine Crystallization applied to MCS Chondrules (Rhodes, 1970).

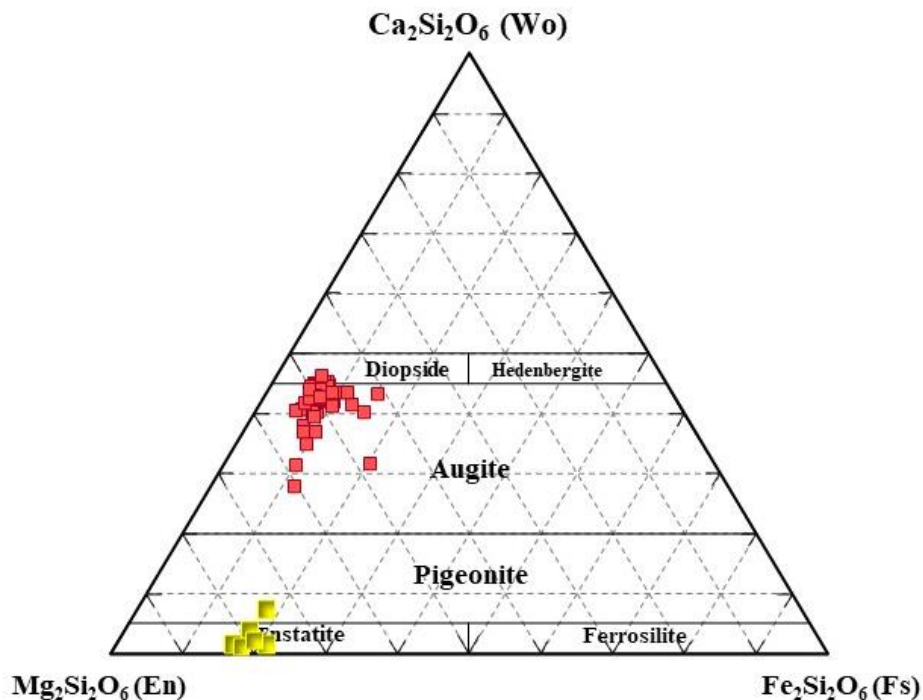


**Figure 5:** Ca-Fe-Mg Pyroxenes Classification Diagram by Morimoto et al. (1988). Data points highlighted in red represent clinopyroxene crystals, while those in yellow denote orthopyroxene crystals. The diagram aids in the systematic classification and differentiation of MCS' pyroxene compositions based on their Ca, Fe, and Mg content.

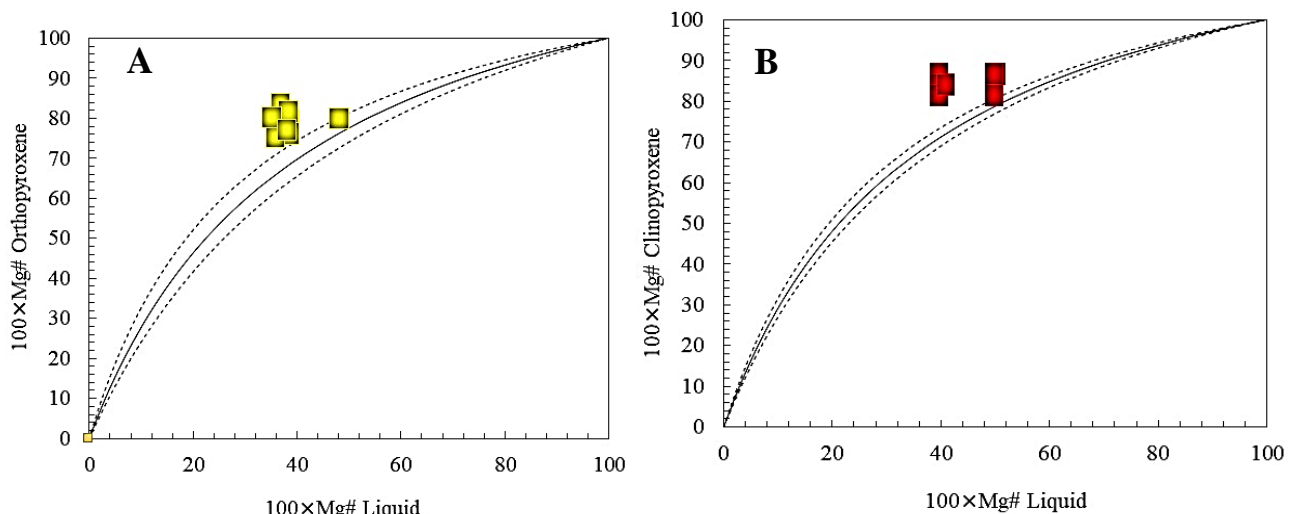


**Figure 6:** Rhodes Diagram for (A) Enstatite and (B) Augite Crystal Composition Data in MCS. The diagram aids in visualizing and comparing the equilibrium with the liquid during the crystallization process for these distinct mineral compositions.

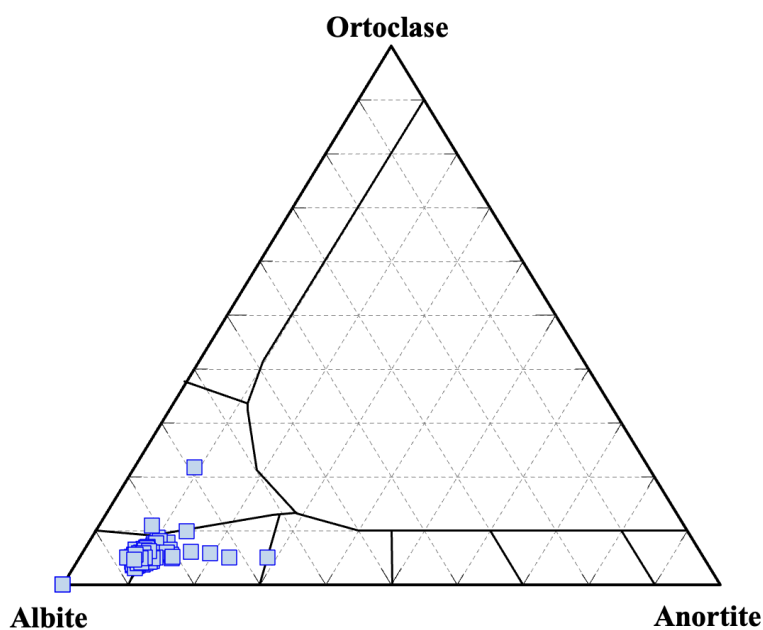


**Figure 7:** Ab-Or-An Classification Diagram Applied to Plagioclase Crystals in the Campos Sales Meteorite. The diagram facilitates the systematic classification of plagioclase compositions based on the abundance of albite (Ab), orthoclase (Or), and anorthite (An), providing valuable insights into the mineralogical characteristics of the meteorite.

Representative samples of 33 chemical compositions from different chondrules are presented in **table 4**. All chondrules, characterized by FeO content exceeding 10%, fall under type II, further subclassified into types A ( $\text{Ol} > 80\%$ ), B ( $\text{Px} > 80\%$ ), or type AB, aligning with observed textural groups (**Tables 5, 6, 7**).

**Table 4:** Chemical Composition of Analyzed Chondrules from the Campos Sales Meteorite, offering comprehensive insights into the elemental makeup of these essential components.

Sample/ Oxide (% wt.)	C21	C23	C22	C28	C32	C26	C17	C8	C25	C16	C18	C6	C5	C4	C20	C1	C2	C11	C12	C3	C31	C9	C10	C30	C33	C19	C7	C24	C29	C13	C15	C27	C14
SiO <sub>2</sub>	40.21	42.81	43.62	43.72	43.75	44.85	44.97	45.72	45.89	45.98	46.39	46.96	47.79	48.05	48.60	48.88	49.08	49.59	50.10	50.65	51.33	51.42	52.87	52.38	53.17	53.38	53.49	53.76	54.21	54.55	54.93	55.42	56.71
TiO <sub>2</sub>	0.05	0.09	0.07	0.07	0.06	0.03	0.04	0.08	0.05	0.06	0.12	0.13	0.09	0.08	0.01	0.17	0.11	0.04	0.14	0.16	0.08	0.13	0.13	0.13	0.13	0.14	0.15	0.14	0.22	0.17	0.19	0.07	0.09
Al <sub>2</sub> O <sub>3</sub>	1.71	4.55	5.05	5.25	3.85	4.97	4.85	5.65	4.20	5.23	11.87	4.40	6.34	6.21	4.99	6.33	6.43	9.08	10.85	5.07	4.75	11.44	3.67	5.36	5.15	7.19	5.36	4.52	5.65	3.60	5.56	4.51	0.12
FeO	18.56	16.66	15.75	16.27	16.09	15.28	14.75	14.50	15.37	14.13	13.65	14.87	13.20	12.98	13.36	13.69	13.50	10.72	10.44	12.94	13.37	9.87	11.45	11.98	11.03	10.27	10.34	11.51	9.00	9.65	10.09	10.07	10.95
MnO	0.39	0.19	0.29	0.35	0.35	0.25	0.32	0.38	0.38	0.29	0.28	0.27	0.28	0.33	0.35	0.28	0.30	0.24	0.26	0.31	0.31	0.19	0.35	0.34	0.34	0.20	0.36	0.30	0.32	0.31	0.28	0.43	0.43
MgO	37.78	27.12	31.90	31.02	32.99	27.72	29.66	29.29	28.69	26.97	19.60	25.44	24.50	28.42	28.16	26.02	26.00	22.05	19.71	26.81	25.25	19.86	27.07	24.75	25.20	16.34	25.42	24.38	20.60	23.92	22.97	23.45	30.83
CaO	0.75	1.52	1.22	0.53	1.26	2.62	3.06	1.36	2.33	4.30	1.29	3.29	2.13	1.25	1.36	1.49	1.45	3.42	1.85	0.94	1.06	1.26	2.55	2.39	2.23	8.32	2.24	1.14	6.64	4.97	2.92	3.82	0.65
Na <sub>2</sub> O	0.43	1.73	1.78	1.99	1.46	2.00	2.01	2.18	1.62	2.32	5.24	1.63	2.47	2.31	2.09	2.34	2.39	4.00	4.68	2.17	1.87	5.09	1.50	2.08	2.11	3.51	1.97	1.71	2.13	1.56	2.33	1.85	0.11
K <sub>2</sub> O	0.05	0.10	0.14	0.18	0.14	0.14	0.16	0.16	0.11	0.17	0.37	0.12	0.19	0.17	0.21	0.19	0.32	0.41	0.16	0.18	0.34	0.09	0.16	0.21	0.26	0.15	0.19	0.19	0.11	0.19	0.15	0.06	
P <sub>2</sub> O <sub>5</sub>		0.08			0.05	0.03	0.33		0.09	0.12		0.06		0.35			0.06				0.28								0.02				
SO <sub>3</sub>	0.04	5.10	0.13	0.56		2.05	0.16	0.26	1.32	0.46	0.97	2.81	2.89	0.15	0.48	0.55	0.50	0.47	1.53	0.79	1.80	0.02	0.24	0.38	0.38	0.39	0.53	2.36	1.05	1.13	0.43	0.23	
Cl	0.03	0.06	0.04	0.05	0.05	0.04		0.07	0.04		0.08	0.07	0.05	0.04	0.04	0.03	0.04		0.03			0.10	0.08	0.04	0.04					0.03	0.05		0.04
<b>Total</b>	100.00	99.99	100.00	100.00	100.00	100.00	100.00	99.99	100.00	100.00	99.98	100.00	99.99	99.99	100.00	100.00	100.00	100.00	100.00	100.00	99.99	99.99	100.00	100.00	100.00	100.00	100.00	99.99	100.00	100.00	100.00		

**Table 5:** Chemical Composition Data for All Type IIA Olivine Chondrules categorized as Granular Olivine (GO) in the Campos Sales meteorite. The data offers detailed insights into the elemental makeup of these specific chondrule types.

Sample/ Oxide (% wt.)	C22	C32	C17	C16	C6	C5	C1	C2	C3	C30	C19	C24	C15	C14
SiO <sub>2</sub>	43.62	43.75	44.97	45.98	46.96	47.79	48.88	49.08	50.65	52.38	53.38	53.76	54.93	56.71
TiO <sub>2</sub>	0.07	0.06	0.04	0.06	0.13	0.09	0.17	0.11	0.16	0.13	0.14	0.14	0.19	0.09
Al <sub>2</sub> O <sub>3</sub>	5.05	3.85	4.85	5.23	4.40	6.34	6.33	6.43	5.07	5.36	7.19	4.52	5.56	0.12
FeO	15.75	16.09	14.75	14.13	14.87	13.20	13.69	13.50	12.94	11.98	10.27	11.51	10.09	10.95
MnO	0.29	0.35	0.32	0.29	0.27	0.28	0.28	0.30	0.31	0.34	0.20	0.30	0.28	0.43
MgO	31.90	32.99	29.66	26.97	25.44	24.50	26.02	26.00	26.81	24.75	16.34	24.38	22.97	30.83
CaO	1.22	1.26	3.06	4.30	3.29	2.13	1.49	1.45	0.94	2.39	8.32	1.14	2.92	0.65
Na <sub>2</sub> O	1.78	1.46	2.01	2.32	1.63	2.47	2.34	2.39	2.17	2.08	3.51	1.71	2.33	0.11
K <sub>2</sub> O	0.14	0.14	0.16	0.17	0.12	0.19	0.21	0.19	0.16	0.26	0.19	0.19	0.06	
P <sub>2</sub> O <sub>5</sub>			0.03	0.09		0.06							0.02	
SO <sub>3</sub>	0.13		0.16	0.46	2.81	2.89	0.55	0.50	0.79	0.38	0.39	2.36	0.43	
Cl	0.04	0.05			0.07	0.05	0.03	0.04		0.04			0.05	0.04
<b>Total</b>	100.00	100.00	100.00	100.00	100.00	99.99	100.00	100.00	100.00	100.00	100.00	100.00	99.99	100.00

**Table 6:** Chemical Composition Data for All Type IIA Olivine Chondrules categorized as Barred Olivine (BO) in the Campos Sales meteorite. The data offers detailed insights into the elemental makeup of these specific chondrule types.

Sample/ Oxide (% wt.)	C21	C28	C26	C4	C12	C9	C10	C33	C7
SiO <sub>2</sub>	40.21	43.72	44.85	48.05	50.10	51.42	52.87	53.17	53.49
TiO <sub>2</sub>	0.05	0.07	0.03	0.08	0.14	0.13	0.13	0.13	0.15
Al <sub>2</sub> O <sub>3</sub>	1.71	5.25	4.97	6.21	10.85	11.44	3.67	5.15	5.36
FeO	18.56	16.27	15.28	12.98	10.44	9.87	11.45	11.03	10.34
MnO	0.39	0.35	0.25	0.33	0.26	0.19	0.35	0.34	0.36
MgO	37.78	31.02	27.72	28.42	19.71	19.86	27.07	25.20	25.42
CaO	0.75	0.53	2.62	1.25	1.85	1.26	2.55	2.23	2.24
Na <sub>2</sub> O	0.43	1.99	2.00	2.31	4.68	5.09	1.50	2.11	1.97
K <sub>2</sub> O	0.05	0.18	0.14	0.17	0.41	0.34	0.09	0.21	0.15
P <sub>2</sub> O <sub>5</sub>			0.05			0.28			
SO <sub>3</sub>	0.04	0.56	2.05	0.15	1.53	0.02	0.24	0.38	0.53
Cl	0.03	0.05	0.04	0.04	0.03	0.10	0.08	0.04	
<b>Total</b>	<b>100.00</b>	<b>100.00</b>	<b>100.00</b>	<b>99.99</b>	<b>100.00</b>	<b>99.99</b>	<b>99.99</b>	<b>100.00</b>	<b>100.00</b>

**Table 7:** Chemical Composition Data for Type IIA Pyroxene Chondrules, specifically categorized as Granular Olivine Pyroxene (GOP), Granular Pyroxene (GP), and Radial Pyroxene (RP) in the Campos Sales meteorite. The data offers comprehensive insights into the elemental makeup of these specific chondrule types.

Type	IIAB - GOP			IIB - GP			IIB - RP		
	Sample/Oxide (% wt.)	C25	C31	C27	C11	C29	C23	C8	C18
SiO <sub>2</sub>	45.89	51.33	55.42	49.59	54.21	42.81	45.72	46.39	48.60
TiO <sub>2</sub>	0.05	0.08	0.07	0.04	0.22	0.09	0.08	0.12	0.01
Al <sub>2</sub> O <sub>3</sub>	4.20	4.75	4.51	9.08	5.65	4.55	5.65	11.87	4.99
FeO	15.37	13.37	10.07	10.72	9.00	16.66	14.50	13.65	13.36
MnO	0.38	0.31	0.43	0.24	0.32	0.19	0.38	0.28	0.35
MgO	28.69	25.25	23.45	22.05	20.60	27.12	29.29	19.60	28.16
CaO	2.33	1.06	3.82	3.42	6.64	1.52	1.36	1.29	1.36
Na <sub>2</sub> O	1.62	1.87	1.85	4.00	2.13	1.73	2.18	5.24	2.09
K <sub>2</sub> O	0.11	0.18	0.15	0.32	0.19	0.10	0.16	0.37	0.21
P <sub>2</sub> O <sub>5</sub>				0.06		0.08	0.33	0.12	0.35
SO <sub>3</sub>	1.32	1.80	0.23	0.47	1.05	5.10	0.26	0.97	0.48
Cl	0.04					0.06	0.07	0.08	0.04
<b>Total</b>	<b>100.00</b>	<b>100.00</b>	<b>100.00</b>	<b>100.00</b>	<b>100.00</b>	<b>99.99</b>	<b>99.99</b>	<b>99.98</b>	<b>100.00</b>

Despite petrographic variations and diverse chemical compositions, attempts to differentiate groups using binary diagrams proved challenging. A positive correlation between sodium and potassium (**Figure 8**) highlights their substitution within plagioclase. Additionally, three main groups, rich in alkalis, intermediate, and low content, are observed independently of textural types, providing further insights into the chemical intricacies of the meteorite.

A notable diversity in composition exists both within and among the studied chondrule groups, featuring ranges of  $\text{SiO}_2 = 33.95\% - 53.86\%$ ,  $\text{MgO} = 15.84\% - 37.28\%$ ,  $\text{FeO} = 8.26\% - 18.31\%$  and  $\text{CaO} = 0.5\% - 8.14\%$ . This compositional variability aligns with expectations when considering the distinct types of chondrules and their mineralogical compositions. In contrast, other assessed chemical elements exhibit percentages within the ranges of  $0.01 < \text{TiO}_2 < 0.2\%$ ,  $0.11 < \text{Al}_2\text{O}_3 < 10.75\%$ , and  $0.17 < \text{MnO} < 0.41\%$ . Consequently, it proved challenging to establish a specific compositional range for these elements based on their association with the identified textural types. Alkali elements, especially  $\text{Na}_2\text{O}$  ( $0.1\% - 4.78\%$ ) and  $\text{K}_2\text{O}$  ( $0.05\% - 0.36\%$ ), vary significantly, they primarily signify the presence of plagioclase in chondrules. Diagrams incorporating  $\text{MgO}$  as a distinguishing agent (**Figure 9**) likely capture the substitution of  $\text{MgO}$  by  $\text{FeO}$  and  $\text{MnO}$  within the olivine and enstatite structures.

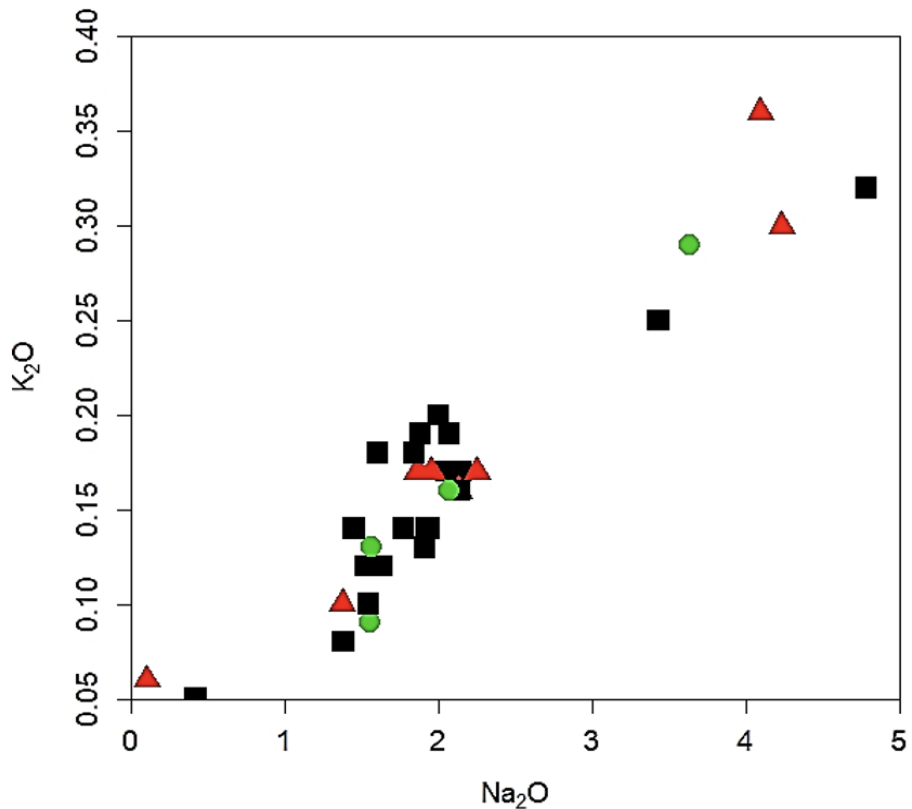


**Figure 8:** Binary Diagram of  $\text{Na}_2\text{O}$  versus  $\text{K}_2\text{O}$  applied to MCS' chondrule compositions obtained in this study. The data points for radial pyroxene chondrules are highlighted in green, barred olivine chondrules in red, and granular chondrules in black. The diagram provides a visual representation of the variations in sodium and potassium oxide content across different chondrule types.

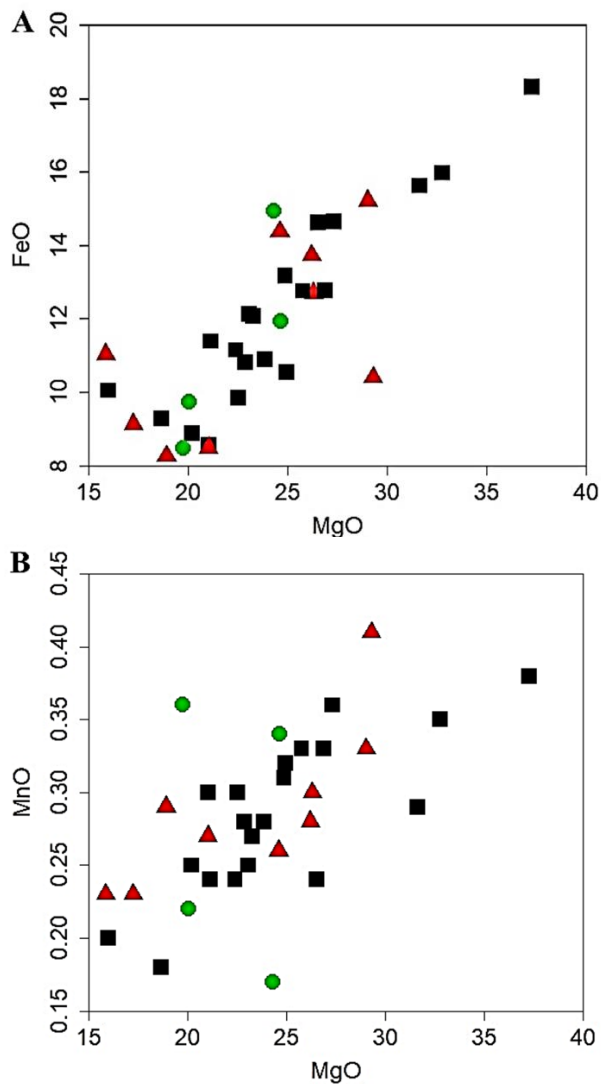


**Figure 9:** MgO versus FeO (A) and MgO versus MnO (B) variation diagrams applied to the compositions of MCS' chondrules. Data points for radial pyroxene chondrules are depicted in green, barred olivine chondrules in red, and granular chondrules in black. The diagrams offer insights into the variations in magnesium, iron, and manganese oxide content across different chondrule types in the study.

## DISCUSSIONS: MINERALOGICAL AND TEXTURAL INSIGHTS IN TYPE L CHONDRULES

### Chondrules Characteristics in Campos Sales Meteorite: Comparisons and Patterns

The mineral chemistry data derived from the Campos Sales meteorite (MSC) sheds light on the homogeneity in the chemical composition of the chondrules examined. A comparative analysis involving olivine ( $\text{Fo}_{75}\text{Fa}_{25}$ ) and orthopyroxene ( $\text{Fs}_{22}$ ) compositions reveals analogous trends with Varre-Sai ( $\text{Fo}_{75}\text{Fa}_{25}$ , VS, Zucolotto et al., 2012) and Lavras do Sul ( $\text{Fo}_{75.1}\text{Fa}_{24.9}$ , LS, Zucolotto et al., 2010) meteorites, both categorized as L5 ordinary chondrites.

Non-porphyritic chondrules in the MCS primarily fall into the categories of barred olivine, radial pyroxene, and granular, aligning with Rubin's (1989a) textural classifications. Similar observations exist in Varre-Sai and Lavras do Sul meteorites, suggesting consistent patterns in L5

ordinary chondrites. No discernible correlation is observed between the size, textural type, and shape of chondrules in MCS. This variability, consistent with previous studies on L-type chondrites (Gooding and Keil, 1981, Gooding, 1983), challenges the notion of strict relationships between these parameters.

Despite some flattened or deformed areas, chondrules' shapes in MCS predominantly exhibit a spherical tendency (**Figure 2C**), especially in radial and barred categories. Gooding and Keil (1981) note that non-porphyritic chondrules often display enhanced sphericity, facilitating their identification during microscopy, and indicative of uniform pressure during their formation. Beyond the presence of rounded chondrules, the MCS exhibits a variety of chondrules with diverse shapes. These include representations of chondrule fragments and granular chondrules. Zucolotto et al. (2012) have previously noted that numerous types of non-porphyritic chondrules and fragments within meteorites, such as the MCS, demonstrate deviations from the expected sphericity pattern.

#### *Deformation and Agglutination Dynamics*

Microscopic examination reveals deformed areas, especially at chondrule boundaries in contact zones, been it is noticeable that chondrules are partially to completely deformed, and even broken at their edges. Ductile deformation of chondrules throughout various types suggests a non-simultaneous crystallization process during agglutination. This evidence aligns with the concept of plastic deformation during the interaction of chondrules in different stages of solidification.

In the MCS context, the observation of ductile deformation across various chondrule types implies that their crystallization did not occur simultaneously during the agglutination phase. Essentially, some chondrules were already in a more solid state, while others exhibited more plastic behavior. The interaction between these chondrules likely led to the deformation of the more plastic ones as they were "pressed" against the more solid ones. As per the findings of Gooding and Keil (1981), the presence of these areas suggests a process of plastic deformation occurring on surfaces that were not entirely solidified, especially when in contact with chondrules in a more advanced stage of solidification.

Deformed areas, as those observed in MCS' chondrules, may also signify shock metamorphism events, evidenced by broken chondrule boundaries. However, determining the timing of these shock events remains challenging, leaving open the question of when these metamorphic events occurred.

#### *Skeletal Olivine and Pyroxenes: Insights into Solar System Origins*

The chondrules examined in the MCS exhibit a notable abundance of skeletal olivine and pyroxenes. This prevalence of specific mineral textures suggests that during the early stages of the Solar System, there were distinct occurrences when materials rich in magnesium and iron formed. Subsequently, these materials underwent rapid crystallization, albeit not necessarily simultaneously. This hypothesis finds support in the work of Blander (1983), which proposes that the origin of chondrules is rooted in the condensation of drops from a metastable silicate liquid, followed by processes of crystallization and accretion. However, it is essential to clarify that these observations do not imply that the chondrules originated from the fractional crystallization of the same magma. Rather, they highlight moments when drops of liquids with specific compositions formed, cooled, and eventually became integral components of the same parental body.

#### **Mineralogical Aspects of Chondrules in L-type Meteorites**

The chemical data for each mineral in MCS reveal minimal compositional variability (**Tables 2 and 3**), implying the classification of this meteorite as a balanced chondrite. Nevertheless, individual chondrules within the meteorite exhibit distinct chemical compositions. Considering these observations, it is plausible to infer the occurrence of a thermal event that prompted chemical reequilibration and suggests diverse sources for the origin of these chondrules.

As elucidated by Blander (1983), variations in composition may arise from kinetic factors such as nucleation constraints during the condensation and crystallization phases, slow chemical reactions, and sluggish ion diffusion rates. Moreover, the possibility of chondrules "inheriting" materials from pre-existing chondrules cannot be discounted. The proposition by Blander (1983) gains support from studies conducted by Ushikubo et al. (2013), particularly those involving oxygen isotopes. These studies indicate discernible differences in nebular compositions during chondrule formation processes for certain types of chondrites.

#### *Unraveling the Significance of Metastable Phases in Chondrules*

In all investigated chondrules within the MCS, a distinctive metastable phase is discernible, characterized by elevated levels of alkalis, silicon, magnesium, iron, and calcium. This phase exhibits compositional similarities to plagioclase and augite, alternating between the two compositions. Primarily occupying interstitial spaces between olivine and enstatite crystals, occasional euhedral inclusions of chromite may be present. Petrographic scrutiny reveals diffuse contacts between plagioclase and augite crystals within this phase, alongside small anhedral crystals of enstatite and olivine interspersed within the interstitial material.

This particular association is not exclusive to the MCS meteorite but is also observed in the Lavras do Sul meteorite (Zucolotto et al., 2010). The metastable phase exhibits various possibilities, including:

- (i) Representing a metastable phase evolving through the exsolution of plagioclase and augite, culminating in a mesh texture. However, the crystals are of such small size that obtaining individual analyses with the SEM beam was unattainable; or
- (ii) Arising from the eutectoid co-crystallization of plagioclase and augite.

In either case, several crystals analyzed within this phase exhibited plagioclase composition. The plagioclase in MCS comprises submillimeter-sized crystals with minimal compositional variation, primarily classified as albite-oligoclase based on chemical data in this study.

The presence of oligoclase is further substantiated by the alkali content in the comprehensive chemical analyses of the chondrules. Alexander et al. (2008) conducted a study on the occurrence of volatile elements, including sodium, in chondrites. According to these authors, the abundance of volatiles remained relatively constant even during the formation of chondrules. To prevent evaporation, the chondrules that preserved these volatile elements would need to originate in regions characterized by high dust/gas ratios. An alternative proposition by Yurimoto and Wasson (2002) suggests that the ratios of sodium and other volatile elements could have been preserved through processes involving rapid fusion and crystallization of the chondrules.

Chen and Goresy (2000) propose in their research that the plagioclase-like material may be maskelynite. Maskelynite, as defined by Chen and Goresy (2000), is a glass with a composition closely resembling that of plagioclase and results from melting caused by a high-pressure episode. Alternatively, the plagioclase might be the high-pressure polymorph of feldspar, known as lingunite, which occurs under conditions of 22 GPa pressure and 2200°C temperature (Liu, 2006).

Among these possibilities, the first aligns most consistently with the textural and chemical data, given the holocrystalline nature of the MCS and the absence of significant indications of shock events in other crystalline phases, such as olivine.

#### *Polymorphs of Chromium*

The euhedral chromium-rich crystals, primarily located within the metastable phase, were initially identified as chromite crystals. Another potential mineral phase, as proposed by Chen et al. (2008) and Xie et al. (2011), suggests that these Cr-crystals may be xieite. Xieite is recognized

as a high-pressure and high-temperature polymorph of chromite, forming under conditions of 20–23 GPa pressure and temperatures between 1800°C and 2000°C.

While the possibility of these crystals being xieite is intriguing, a comprehensive assessment reveals the absence of other minerals exhibiting textures indicative of a high-intensity shock event. According to the criteria established by Stöffler et al. (1991), the shock levels in MCS are classified as S1-S2, denoting a very weak shock experience with impact pressures ranging from 4 to 10 GPa and a post-shock temperature increase between 10 and 50°C. Given these considerations, it is presently more appropriate to assert that the crystals within the metastable phase are, indeed, chromite.

#### *Geothermometry*

Utilizing olivine crystals as a basis, the geothermometer proposed by Putirka (2008) yields temperatures ranging from 1076.78°C to 1125.38°C. Similarly, when the geothermometer developed by Putirka et al. (1996) is applied to enstatite crystals, it indicates a temperature range akin to that of olivine, with values spanning from 973.65°C to 1126.94°C. The geothermometer values for olivine align closely with those suggested by Murata et al. (2007) for the crystallization temperatures of this mineral. Furthermore, in the context of L-type chondrites, where thermal events are concerned, Slater-Reynolds & McSween (2005) propose a maximum temperature of 950°C.

Notably, no discernible textural features indicative of a significant thermal metamorphic event was identified in the MCS. Consequently, it is inferred that the calculated values aptly represent the crystallization temperatures of the examined minerals.

## CONCLUSIONS

Grounded in the premise that chondrules might embody droplets derived from distinct magmas formed during the early phases of the Solar System, our study delves into 33 chondrules from the Campos Sales meteorite, an L5 ordinary chondrite.

Chondrules within the MCS showcase a composition dominated by skeletal crystals of olivine, enstatite, and augite, accompanied by varying proportions of metal, troilite, plagioclase, chromite, and Cl-apatite. The predominant textural variations include barred, radial, and granular structures.

Analysis of mineral chemical composition data reveals minimal variation within individual crystals. Nevertheless, each chondrule exhibits a distinct composition, suggesting diverse progenitors for these particles. Our interpretation posits that the minerals in MCS chondrules underwent formation via a multitude of processes in their nebular origin region. Differences in these processes and compositions within the nebular zone likely influenced the observed chondrule compositions. Contemporary features affirm the rapid formation of chondrules. During accretion for parental body formation, not all chondrules were fully solidified, resulting in varied chondrule shapes.

The presence of skeletal crystals implies rapid chondrule crystallization, preserving volatile elements, notably within the meta-stable phase rich in olivine crystals. Subsequently, MCS chondrules experienced accretion, forming a larger body. A subsequent thermal event, possibly shock-induced disaggregation, occurred with temperatures and pressures adequate for mineral re-equilibration but insufficient for differentiation or obliteration of most chondrules.

While the homogeneity in crystal composition strongly indicates the occurrence of this thermal event, geothermometric data suggest crystallization temperatures rather than subsequent events. In summary, our comprehensive investigation into the mineralogical and textural facets of type L meteorite chondrules unveils crucial insights into their composition, formation

dynamics, and the potential influence of diverse processes during the early stages of the Solar System.

## ACKNOWLEDGMENT

We extend our sincere gratitude to various entities that played integral roles in the successful completion of this research. The Nucleo de Estudos em Meteoritos / ProMete-UFBA significantly contributed by engaging in discussions that proved vital for meteoritic studies. Their unwavering support greatly enriched the depth and breadth of our investigation. The Brazilian Geological Survey / SUREG-Salvador deserves recognition for their meticulous sample preparation, ensuring the quality and integrity of the materials analyzed in this study. Their expertise in handling meteoritic samples significantly enhanced the precision of our findings. Our heartfelt appreciation goes to the dedicated staff and graduate students of the Condominio de Laboratorios Multiusuarios das Geociencias da Universidade Federal de Sergipe. Their collaborative efforts provided invaluable insights and technical assistance throughout various phases of this research. The financial support from the Coordenação de Aperfeiçoamento de Pessoal de Nível Superior – Brasil (CAPES), under the Financing Code 001, was instrumental in conducting the extensive analyses and experiments essential for this study. A special acknowledgment is reserved for Dr. Wilton Pinto de Carvalho for generously donating the sample that served as the focal point of our investigation and for introducing all authors to the wonders of the Meteoritics. His contribution played a pivotal role in advancing our understanding of meteoritic materials. The synergy of these institutions, coupled with the generous support of individuals, has been instrumental in the success of this research endeavor. We extend our sincere appreciation to all the reviewers who contributed to the fruition of this scientific exploration.

## CONFLICT OF INTEREST DECLARATION

We, the undersigned authors of this paper declare that we have no conflicts of interest to disclose regarding this research. We have not received any financial support or funding, and we have no financial interests, personal relationships, or affiliations with organizations that could be perceived as affecting the research, analysis, or conclusions presented in this paper. We also affirm that we have no competing professional or personal interests that could impact the integrity or impartiality of the research conducted or the findings reported.

## REFERENCES

- Alexander, C.M.O'd., Grossman, J.N., Ebel, D.S., Ciesla, F.L. 2008. The formation conditions of chondrules and chondrites. *Science*. 320, 5883, 1617-1619. <https://doi.org/10.1126/science.1156561>
- Chen M., Goresy A.E. 2000. The nature of maskelynite in shocked meteorites: not diaplectic glass but a glass quenched from shock-induced dense melt at high pressures. *Earth and Planetary Science Letters*. 179, 489-502. [https://doi.org/10.1016/S0012-821X\(00\)00130-8](https://doi.org/10.1016/S0012-821X(00)00130-8)
- Chen, M., Chu, J.F., Mao, H.K. 2008. Xieite, a new mineral of high-pressure FeCr<sub>2</sub>O<sub>4</sub> polymorph. *Chinese Science Bulletin*. 54, 3341-3345.
- Comelli, D., D'Orazio, M., Folco, L., El-Halwagy, M., Frizzi,T., Alberti, R., Capogrosso, V., Elnaggar, A., Hassan, H., Nevin, A., Porcelli, F., Rashed, M.G., Valentini, G. 2016. The meteoritic origin of Tutankhamun's iron dagger blade. *Meteoritics & Planetary Science*. 51, 7, 1301-1309. <https://doi.org/10.1111/maps.12664>

- Desch, S.J., Morris, M.A., Connolly Jr, H.C., Boss, A.P. 2012. The importance of experiments: Constraints on chondrule formation models. *Meteoritics and Planetary Science*. 47, 1139-1156. <https://doi.org/10.1111/j.1945-5100.2012.01357.x>
- Dodd, R. T. 1981. *Meteorites, A Petrologic-chemical Synthesis*. Cambridge University Press, Cambridge.
- Gazillo Neto, R. 2018. Química Mineral e Geotermometria dos Condritos Comuns Campos Sales e Santa Vitória do Palmar. In: Dissertação de Mestrado – Universidade Federal do Ceará, Centro de Ciências, Programa de Pós-graduação em Geologia, 72p.
- Gooding, J.L., Keil, K. 1981. Relative abundances of chondrule primary textural types in ordinary chondrites and their bearing on conditions of chondrule formation. *Meteoritics*. 16, 17-43. <https://doi.org/10.1111/j.1945-5100.1981.tb00183.x>
- Gooding, J. L. 1983. Survey of chondrule average properties in H-, L-, and LL-group chondrites - Are chondrules the same in all unequilibrated ordinary chondrites? In: King, E. A. (Ed.) *Chondrules and their origins*. Lunar and Planetary Institute, Houston, 61-87.
- Grossman, L., Larimer, J.W. 1974. Early Chemical history of the solar system. *Geophysics and Space Physics*. 12, 71-101. <https://doi.org/10.1029/RG012i001p00071>
- Gündüz, M., Asan, K. 2022. MagMin\_PT: An Excel-based mineral classification and geothermobatometry program for magmatic rocks. *Mineralogical Magazine*.
- Hewins R.H. 1997. Chondrules. *Annual Reviews of Earth and Planetary Science*. 25, 61-83. <https://doi.org/10.1146/annurev.earth.25.1.61>
- Johnson, B.C., Minton, D.A., Melosh, H.J., Zuber, M.T. 2015. Impact jetting as the origin of chondrules. *Nature*. 517, 339-341. <https://doi.org/10.1038/nature14105>
- Larimer, J.W. 1967. Chemical fractionations in meteorites: I. Condensation of the elements. *Geochimica et Cosmochimica Acta*. 31, 1215-1238. [https://doi.org/10.1016/S0016-7037\(67\)80013-9](https://doi.org/10.1016/S0016-7037(67)80013-9)
- Larimer, J.W., Anders, E. 1967. Chemical fractionations in meteorites. Part.II: Abundance patterns and their interpretation. *Geochimica et Cosmochimica Acta*. 31, 1239-1270. [https://doi.org/10.1016/S0016-7037\(67\)80014-0](https://doi.org/10.1016/S0016-7037(67)80014-0)
- Libourel, G., Portail, M. 2018. Chondrules as direct thermochemical sensors of solar protoplanetary disk gas. *Science Advances*. 4, eaar3221. <https://doi.org/10.1126/sciadv.aar3221>
- Liu, X. 2006. Phase relations in the system  $KAlSi_3O_8-NaAlSi_3O_8$  at high pressure – high temperature conditions and their implication for the petrogenesis of lingunite. *Earth and Planetary Science Letters*. 246, 317-325. <https://doi.org/10.1016/j.epsl.2006.04.016>
- McSween, H. Y., JR.; Sears, D. W. G.; Dodd, R. T. Jr. 1988. Thermal metamorphism; In *Meteorites and the Early Solar System* (eds. J. R. Kerridge and M. S. Matthews), 102 - 113. Univ. Arizona Press, Tucson, Arizona.
- Merrill, G.P. 1920. On chondrules and chondritic structure in meteorites. *Nacional Academy of Sciences of the United States of America*. 6, 8, 449-472.
- Morris, M. A., Weidenschilling, S. J., Desch, S. J. 2016. The effect of multiple particle sizes on cooling rates of chondrules produced in large-scale shocks in the solar nebula. *Meteoritics and Planetary Science*. 51, 870–883. <https://doi.org/10.1111/maps.12631>
- Murata, K., Chihara, H., Tsuchiyama, A., Koike, C., Takakura, T., Noguchi, T., & Nakamura, T. 2007. Crystallization experiments on amorphous silicates with chondritic composition: Quantitative formulation of the crystallization. *The Astrophysical Journal*. 668, 285-293. <https://doi.org/10.1086/521017>

- Putirka, K.; Johnson, M.; Kinzler, R.; Longhi, J.; Walker, D. 1996. Thermobarometry of mafic igneous rocks based on clinopyroxene-liquid equilibria, 0-30 kbar. Contributions to Mineralogy and Petrology. 123, 122-138. <https://doi.org/10.1007/s004100050145>
- Putirka, K. 2008. Thermometers and Barometers for Volcanic Systems. In: Putirka, K., Tepley, F. (Eds.), Minerals, Inclusions and Volcanic Processes, Reviews in Mineralogy and Geochemistry. Mineralogical Society of America. 69, 61-120. <https://doi.org/10.2138/rmg.2008.69.3>
- Rubin, A. E. 1989a. Size-frequency distributions of chondrules in CO<sub>3</sub> chondrites. Meteoritics. 24, 179-189. <https://doi.org/10.1111/j.1945-5100.1989.tb00960.x>
- Rubin, A., Ma, C. 2020. Meteorite Mineralogy. Oxford Research Encyclopedia of Planetary Science. <https://doi.org/10.1093/acrefore/9780190647926.013.205>
- Scorzelli, R.B., Christophe Michel-Lévy, M., Gilabert, E., Lavielle, B., Souza Azevedo, I., Vieira, V.W., Costa, T.V.V., Araújo, M.A.B. 1998. The Campos Sales meteorite from Brazil: a lightly shocked L5 chondrite fall. Meteoritics and Planetary Science. 33, 1335-1337. <https://doi.org/10.1111/j.1945-5100.1998.tb01317.x>
- Scott, E.R.D., Krot, A.N. 2005. Chondrites and their Components. In: HOLLAND, H.D.; TUREKIAN, K.K. Meteorites, Comets and Planets: Treatise on Geochemistry.: Elsevier, v. 1, cap. 107, p. 143-200. ISBN 0080447201.
- Slater-Reynolds, V., McSween Jr, H. Y. 2005. Peak metamorphic temperatures in type 6 ordinary chondrites: An evaluation of pyroxene and plagioclase geothermometry; Meteoritics & Planetary Science. 40, 5, 745 – 754. <https://doi.org/10.1111/j.1945-5100.2005.tb00977.x>
- Urey, H.C. 1954. On the dissipation of gas and volatilized elements from protoplanets. Astrophysics Journal. 1, 147-173.
- Ushikubo, T., Nakashima, D., Kimura, M., Tenner, T.J., Kita, N.T. 2013. Contemporaneous formation of chondrules in distinct oxygen isotope reservoirs. Geochimica et Cosmochimica Acta. 109, 280-295. <https://doi.org/10.1016/j.gca.2013.01.045>
- Xie, X.D., Chen, M., Wang, C.Y. 2011. Occurrence and mineral chemistry of chromite and xieite in the Suizhou L6 chondrite. Science China Earth Sciences. 54, 998-1010.
- Warr, L.N. 2021. IMA-CNMNC approved mineral symbols. Mineralogical Magazine. 85, 291-320. <https://doi.org/10.1180/mgm.2021.43>
- Wang, K., Korotec, R. 2019. Meteorites. Oxford Research Encyclopedia of Planetary Science. <https://doi.org/10.1093/acrefore/9780190647926.013.16>
- Wang, X., Hou, T., Wang, M., Zhang, C., Zhang, Z., Pan, R., Marxer, F., Zhang, H. 2021. A new clinopyroxene thermobarometer for mafic to intermediate magmatic systems. Eur. J. Mineral. 33, 621-637. <https://doi.org/10.5194/ejm-33-621-2021>
- Wood, J.A. 1963. On the origin of chondrules and chondrites. Icarus. 2, 152-180.
- Yurimoto H. And Wasson J. T. (2002) Extremely rapid cooling of a carbonaceous-chondrite chondrule containing very 16O-rich olivine and a 26Mg excess. Geochimica et Cosmochimica Acta. 66, 4355–4363. [https://doi.org/10.1016/S0016-7037\(02\)01218-8](https://doi.org/10.1016/S0016-7037(02)01218-8)
- Zanda, B. 2004. Chondrules. Earth and Planetary Science Letters. 224, 1-17. <https://doi.org/10.1016/j.epsl.2004.05.005>
- Zucolotto, M. E., Antonello, L.L., Varela, M.E., Scorzelli, R.B., Ludka, I.P., Munayco, P., Santos, E. 2010. Lavras do Sul: A new equilibrated Ordinary L5 chondrite from Rio Grande do Sul, Brazil. Meteoritics and Planetary Science Supplement. <https://doi.org/10.1007/s11038-011-9385-4>

Zucolotto, M. E., Antonello, L.L., Varela, M.E., Scorzelli, R.B., Munayco, P., Santos, E., Ludka, I.P. 2012. Varre-Sai: The recente brazillian fall. *Earth, Moon, and Planets*. 109, 43-53.  
<https://doi.org/10.1007/s11038-012-9401-36>

## **CAPÍTULO III: CONCLUSÕES**

## CONCLUSÕES

A partir das evidências e discussões aqui apresentadas fica claro que os meteoritos representam parte fundamental da história do Sistema Solar, que ainda não é completamente conhecida pela humanidade. O que se pode argumentar, até aqui, é que o conhecimento sobre os materiais primordiais formados nos primeiros estágios evolutivos do Sistema Solar, é essencial para avançar na compreensão dos processos que culminaram em sua atual configuração, os quais permanecem intrigantemente desconhecidos. Ademais, é a partir do estudo de meteoritos condrícticos que é possível entender uma das primeiras estruturas geradas com o resfriamento da nebulosa solar: os côndrulos.

Os côndrulos são partículas submilimétricas a milimétricas, com formas arredondadas e compostas por silicatos ferromagnesianos. É a partir do estudo desses minerais máficos e das relações entre eles, que é possível vislumbrar os processos, o tempo, e as condições vigentes e que resultaram nas rochas extraterrestres de onde os côndrulos são encontrados hoje.

A partir da proposição da hipótese investigativa em que se considera os côndrulos como possíveis gotas de “magmas” nebulares, buscou-se conhecer aspectos peculiares a essas partículas. A base deste estudo foi a investigação textural, mineral e química dos côndrulos presentes no meteorito Campos Sales (MCS).

Os tipos texturais majoritários de côndrulos do MCS são: barrado, radial e granular. Esses côndrulos costumam ter formas que tendem a esfera, podendo ou não apresentar áreas deformadas quando em contato com outros. Além disso, essas feições texturais são as mais distinguíveis e preservadas em comparação com a matriz do meteorito.

Os côndrulos do MCS são compostos predominantemente por cristais esqueléticos de olivina ( $\text{Fa}_{25}\text{Fo}_{75}$ ) e enstatita ( $\text{En}_{75-79}, \text{Fs}_{25-21}$ ), e secundariamente por cristais de augita e plagioclásio os quais apresentam texturas que sugerem processos de ex-solução. Adicionalmente, foi possível identificar cristais submilimétricos euedrais de cromita/xieita, dispersos entre os cristais de plagioclásio e augita, bem como cristais de Cl-apatita.

Chama a atenção a existência de microesferas de dióxido de silício, também associadas com os cristais de plagioclásio dentro dos côndrulos de olivina barrada. Tais esferas são

raras e, na amostra estudada do MCS, foi possível observar apenas 3 destas esferas, com tamanho sempre inferior a 0,005 mm.

Salienta-se aqui o fato de que cristais de troilita e liga Fe-Ni são encontrados, por vezes, inclusos em côndrulos granulares e radiais, mas não é tão corriqueiro encontrá-los em côndrulos barrados. Dessa maneira, sua maior presença é na matriz do meteorito, principalmente nas adjacências dos côndrulos.

Tendo em vista os aspectos compositionais, os minerais que compõem os côndrulos do MCS apresentam pouca variação centro-borda. Esse aspecto confirma a classificação da amostra como um condrito ordinário reequilibrado, além de indicar a existência de um evento termal que tenha propiciado o reequilíbrio composicional.

Os dados químicos permitiram não apenas a classificação dos cristais de olivina, enstatita e augita, mas também foram utilizados para classificar o plagioclásio. Apesar dos cristais de plagioclásio serem muito pequenos ( $<30\mu\text{m}$ ), os teores de sódio associados aos baixos conteúdos de potássio e cálcio permitem determinar sua composição como de oligoclásio.

Mediante aos aspectos interpretadas a partir do desafio proposto pelo estudo dos côndrulos do MCS, apresenta-se as etapas relacionadas à sua história de formação, desde suas origens até a sua chegada à superfície da Terra. Estas fases podem ser sumariadas como:

- (1) Formação dos côndrulos a partir do resfriamento rápido do material nebular precursor;
- (2) Acresção dos côndrulos em diferentes estágios de resfriamento e formação do corpo parental;
- (3) Ocorrência do evento termal e reequilíbrio químico;
- (4) Chegada a Terra.

Apesar dessas etapas parecerem óbvias, muito ainda se desconhece sobre os mecanismos que desencadearam essas fases. Alguns autores apontam que a formação dos diferentes côndrulos indica a variabilidade de composição entre as regiões nebulares. Mediante à variação de composição química e as diferentes texturas encontradas acredita-se que a ideia sobre a formação esteja correta e seja representativa para o conjunto amostral estudado. Sugere-se, pois, a continuidade das pesquisas com a integração de dados isotópicos.

## **ANEXOS**

## Estado da Arte

Os meteoritos são a principal fonte de informação sobre a composição dos materiais extraterrestres (Palme & Zipfel, 2017). Esses fragmentos de rocha – ou metal – são originados principalmente a partir de colisões dos corpos asteroidais ou planetesimais presentes no cinturão de asteroides, e, secundariamente, da superfície da Lua e de Marte (Engrand, 2011; Palme & Zipfel, 2017). Eles, também são compostos de assembleias complexas de minerais anidros e hidratados, podendo ter ou não algum composto orgânico (Engrand, 2011).

A classificação dos meteoritos agrupa de amostras que experimentaram processos similares na formação de seus corpos parentais de origem, contudo esse aspecto não quer dizer diretamente que amostras de um mesmo grupo pertençam a apenas um único corpo parental. (Engrand, 2011). Existem dois grandes grupos de meteoritos: (i) diferenciados – rochosos acondríticos, férreos magnéticos e mistos – e (ii) não diferenciados – rochosos condrílicos (Figura 11), os quais se subdividem em diversos outros subgrupos (Zanda, 2004; Engrand, 2011; Jacquet, 2022), sistematizados na figura abaixo.

## Grupos de Meteoritos

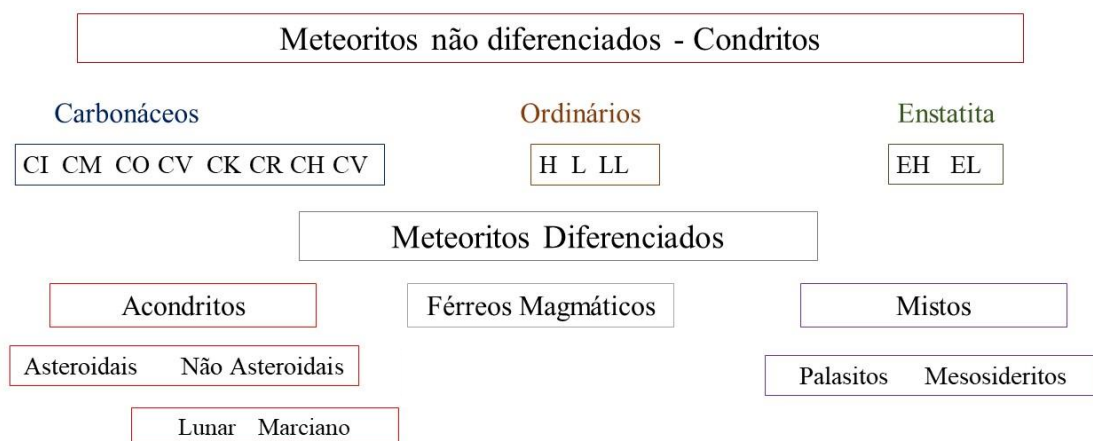


Figura 11. Esquema simplificado de classificação dos meteoritos. Tradução da autora a partir da imagem disposta no trabalho de Jacquet (2022). Carbonáceos: meteorito de Ivuna (CI); meteorito de Mighei (CM); meteorito de Ornans (CO); meteorito de Vigarano (CV); meteorito de Karoonda (CK); meteorito de Renazzo (CR); meteorito carbonáceo com >50% de FeNi. Ordinários: meteoritos com 25 - 30% de teor de ferro (H); meteoritos com 20 – 25% de teor de ferro (L); meteoritos com teor de ferro <20% (LL). Enstatita: alto teor de ferro (EH); baixo teor de ferro (EL).

A classificação simplificada apresentada na Figura 1 evidencia que os meteoritos diferenciados são originados a partir de corpos parentais que sofreram diferenciação química, que experimentaram fusão, e tiveram seus constituintes químicos dispostos em uma estrutura acamada – núcleo, manto e crosta (Palme & Zipfel, 2017) – como é o caso do planeta Terra. É por isso que essas rochas constituem amostras essenciais para o entendimento dos processos de formação planetária (Engrand, 2011).

Os acondritos, por exemplo, apresentam composições bastante diferentes da composição média do sistema solar, em função dos processos de diferenciação ocorridos nos corpos parentais (Palme & Zipfel, 2017), sendo correlacionáveis às camadas mais externas da litosfera dos planetas rochosos.

Em se tratando dos meteoritos não diferenciados, essas rochas são oriundas de corpos que não experimentaram processos de diferenciação, pois não alcançaram temperaturas altas o suficiente para se fundirem totalmente. Nesse grupo, encontram-se as rochas chamadas de condritos (Palme & Zipfel, 2017).

Desta forma, as amostras condríticas podem ser consideradas as mais primitivas em termos de composição, uma vez que apresentam teores elementais próximos à média do sistema solar. Contudo, mesmo os corpos parentais condrícticos experimentaram posteriormente vários graus de metamorfismo termal, correlacionáveis aos impactos que fragmentaram estes planetesimais (Engrand, 2011; Palme & Zipfel, 2017).

Importante citar, no caso do condrito primitivo, a classe dos condritos carbonáceos. Os meteoritos dessa classe experimentaram episódios de alteração aquosa, mas suas composições continuam similares às razões elementares da fotosfera solar, o que indica uma preservação da composição do momento em que tais rochas foram geradas (Lodders, 2010).

Seguindo-se a classificação apresentada na Figura 11, existem três categorias principais para de condritos: os enstatita condritos (EC), os condritos carbonáceos (CC), e os condritos ordinários (OC). Sobre eles seguem-se algumas explicações, respectivamente.

Os EC foram formados em ambientes tão reduzidos que elementos litófilos como manganês e cálcio são presentes em sulfetos. Nessa classe, também existem variações no teor de ferro permitindo uma subclassificação como ELL (muito baixo conteúdo de Fe), EL (baixo conteúdo de Fe) e EH (alto conteúdo de ferro).

Em contrapartida, o grupo dos CC representam os condritos que apresentam algum conteúdo de material orgânico, além de a magnetita, um óxido de Fe, ser

encontrada ao invés da liga metálica (Fe-Ni), comum em meteoritos. Essa categoria apresenta diversos subgrupos que são, em geral, denominados de acordo com o meteorito tipo do grupo, por exemplo: CI – Condrito Ivuna, CM – Condrito Murray, CV – Condrito Vigarano, entre outros.

Por fim, os condritos ordinários (OC = Ordinary Chondrites) integram o grupo dos condritos mais comuns, podendo ser subdivididos de acordo com os teores de ferro em: H (alto teor de Fe – 25 a 30 wt%); L (baixo teor de Fe – 20 a 25 wt%) e LL (baixíssimo teor de Fe <20%) (Zanda, 2004; Oliveira, 2020). A classificação dos OC leva também em consideração a definição física (limites) dos côndrulos presentes, cujo valor varia de 3-6, com o tipo 3 representando condritos com côndrulos muito bem definidos (Figura 12A), e o tipo 6 representando condritos cujos côndrulos são pouco definidos (Figura 12B). Os tipos 1 e 2 são utilizados apenas para a classificação de meteoritos que experimentaram alteração aquosa.

Um dado relevante a acrescentar é de que os condritos, de forma geral, são formados por uma matriz na qual estão presentes côndrulos e outras inclusões refratárias.

Estas inclusões refratárias são compostas de minerais de altas temperaturas (1773-1883°C), sendo os dois tipos principais de inclusões os: silicatos e óxidos ricos em Ca-Al (CAIs) e os agregados de olivina ameboidais (AOA) (Scott e Krot, 2005).

A matriz condríctica se refere a todo o material de granulometria fina que envolve os côndrulos. Os cristais da matriz são compostos de minerais anidros e/ou hidratados com cerca de 10 nm até 5 µm (Brearley, 2005).

Os côndrulos são esferas milimétricas a submilimétricas que correspondem às primeiras gotas de produtos nebulares cristalizadas na forma esférica, e que constituem de 20% – 80% da massa dos condritos (Hewins, 1997; Zanda, 2004; Alexander *et al.*, 2008; Engrand, 2011; Palme & Zipfel, 2017).

Por sua importância para os estudos sobre condritos destaca-se que os côndrulos são predominantemente compostos por silicatos ferromagnesianos (olivina e piroxênios) que experimentaram fusão a partir de um mesmo e desconhecido processo, antes de serem incorporados, por acresção, aos corpos parentais (Hewins, 1997). Por isto mesmo se considera de grande importância avaliar a composição e as texturas presentes nessas partículas para entender quais processos poderiam ser comuns durante os primeiros estágios de formação do Sistema Solar.

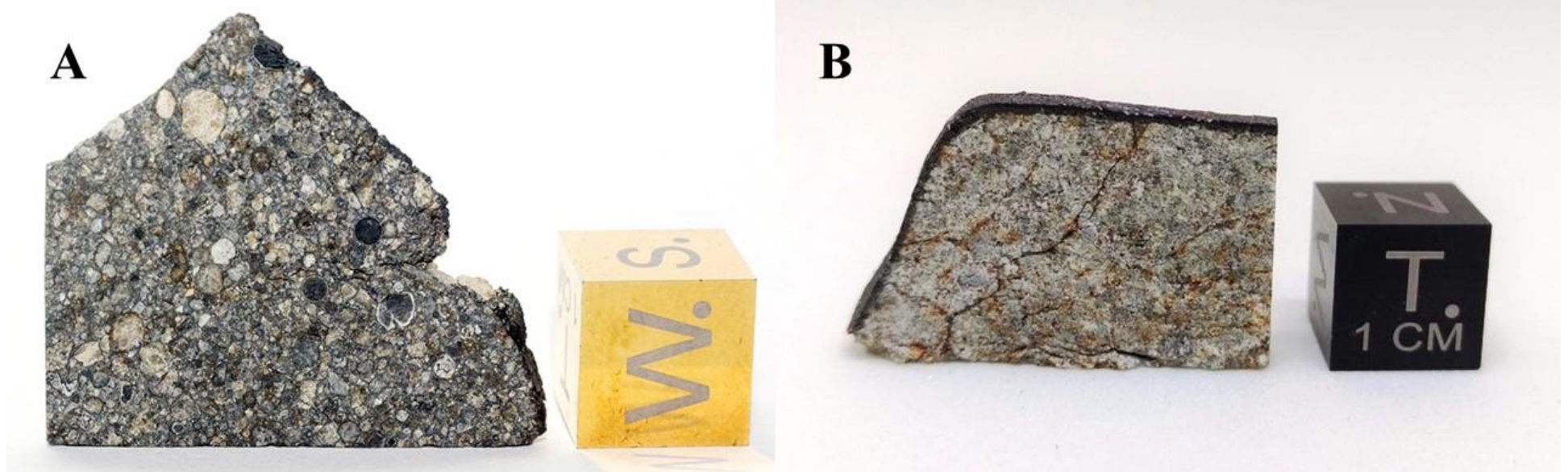


Figura 12. Imagens de fragmentos de condritos ordinários. A- Amostra do condrito ordinário Vicência com as estruturas arredondadas - côndrulos - bastante definidas. Imagem por Anna Morris, disponível em: [https://www.lpi.usra.edu/meteor/get\\_original\\_photo.php?recno=5759274](https://www.lpi.usra.edu/meteor/get_original_photo.php?recno=5759274) visitado no dia 20/03/2023. B- Amostra do condrito Três Irmãos cujos côndrulos não estão distinguíveis a olho nu. Imagem por Rodrigo Guerra, disponível em: [https://www.lpi.usra.edu/meteor/get\\_original\\_photo.php?recno=5760140](https://www.lpi.usra.edu/meteor/get_original_photo.php?recno=5760140) acessado em 20/03/2023.

McSween (1977) reconheceu, dois grupos principais de côndrulos:

- (i) pobres em FeO (tipo I)
- (ii) ricos em FeO (tipo II).

Nessa classificação de McSween (1977), além dos côndrulos, os minerais mais importantes eram a troilita, a liga Fe-Ni e o vidro. Para os côndrulos do tipo I, verificou-se um menor teor de ferro nos silicatos, com a presença do Fe na liga metálica Fe-Ni e no sulfeto. Esse comportamento foi associado com a formação em condições mais reduzidas. Os côndrulos do tipo II que contêm teores mais elevados de Fe nas estruturas da olivina e dos piroxênios, tiveram suas origens associadas a ambientes com condições mais oxidantes.

Posteriormente, Gooding & Keil (1981) tomando como referência os parâmetros de observação para rochas ígneas, sugeriram uma classificação para os côndrulos correlacionando as texturas observadas (barrada, radial, porfirítica, microporfirítica e granular) com o mineral predominante (olivina e/ou piroxênio) (Figura 13).

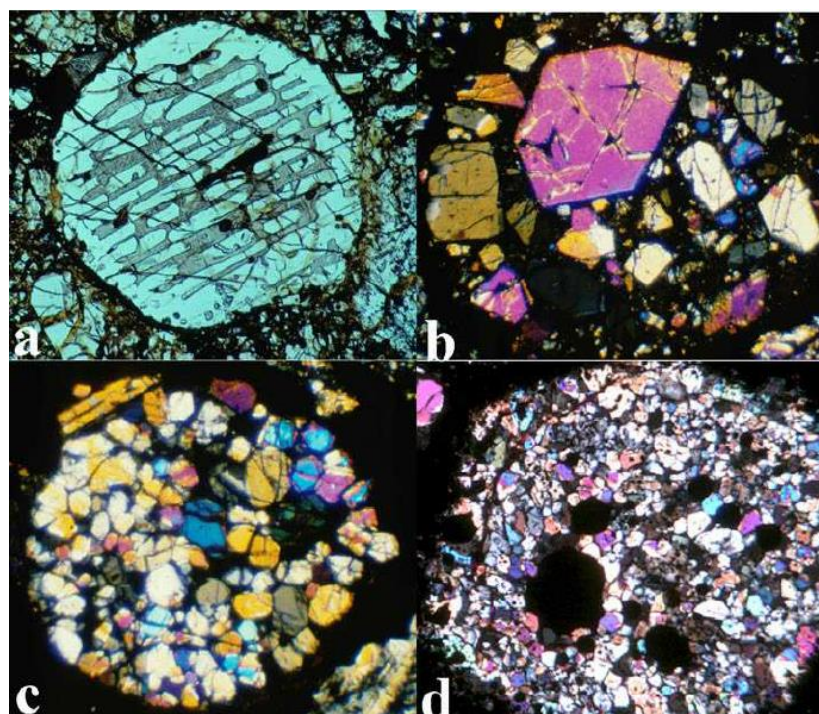


Figura 13. Imagens de texturas em côndrulos obtidas na literatura. A- Côndrulo de olivina barrada; B- Côndrulo de olivina porfirítica; C- Côndrulo de olivina microporfirítica; D- Côndrulo de olivina microporfirítica.. (Hewins, Connolly, Libourel, 2005)

Foi a partir dos trabalhos de McSween (1977), Gooding & Keil (1981) e Jones (1994) que Hewins (1997) associou e resumiu as classificações sugeridas anteriormente na tabela 1, que pode ser vista abaixo.

Tabela 9. Classificação de Côndrulos segundo Hewins (1997). Abreviações: Faialita (Fa), Olivina (Ol), Intermediário (Int.), Piroxênio (Px), Olivina (Ol), Olivina Microporfírica (MPO), Olivina Granular (GO), Olivina Barrada (OB), Olivina Porfirítica (OP), Piroxênio Radial (RP), Piroxênio Porfirítico (PP), Piroxênio Granular (GP), Olivina Piroxênio Radial (POR), Olivina Piroxênio Porfirítica (POP) e Olivina Piroxênio Granular (GOP).

<b>Tipo</b>	<b>Subtipo</b>	<b>Variedades Texturais</b>	
I (pobre em FeO) Olivina Fa<10.	IA	Ol> 80%	MPO, GO, (BO, PO)
	IAB	Int.	POR, POP, GOP
	IB	Px>80%	RP, PP, GP
II (rico em FeO) Olivina Fa>10.	IIA	Ol> 80%	OB, OP, (MPO, GO)
	IIAB	Int.	POR, POP, GOP
	IIB	Px>80%	RP, PP, GP

Baseando-se nos aspectos texturais, Hewins (1988) e Lofgren (1996) inferiram as feições presentes nos côndrulos para inferência dos principais processos ocorridos em sua gênese. Mediante isso, indicou-se que na formação dos cristais esqueléticos de olivina e piroxênio (BO e RP) ocorreu uma fase de crescimento rápido dos cristais. Essa etapa se desenvolveria enquanto os côndrulos ainda estavam totalmente fundidos e começaram a resfriar.

Tratando do tema, Hewins (1997) acrescenta ainda que as relações entre os côndrulos podem esclarecer, ou complicar ainda mais o entendimento sobre os mecanismos que originaram tais partículas. Por exemplo, a existência de côndrulos inclusos nas estruturas de outros, bem como a presença de anéis ígneos, indicam que a formação de tais estruturas condriticas não foi coetânea.

É necessário ter em mente que os estudos sobre a origem dos côndrulos começaram a ocorrer muito antes do século XX. De acordo com Merrill (1920), em 1864 o pesquisador H. C. Sorby, na Inglaterra, indicou que o material de um condrito poderia

ter se originado a partir da fusão, ruptura em partes menores e posterior consolidação a partir de ações mecânicas e químicas do seu corpo parental.

A proposição de Sorby foi validada com a pesquisa de Paque & Bunch (1997). Os dados obtidos por estes autores indicaram que as feições presentes nos côndrulos exigem um evento de aquecimento muito rápido ( $<1600^{\circ}\text{C}$ ), seguido de um evento de resfriamento mais rápido do que o resfriamento nebular. De igual modo, segundo os mesmos autores, após a formação de cada côndrulo, mediante a um mecanismo de acumulação de massa que concentra os côndrulos e os separa por tamanho, inicia-se a acresção que culminaria na formação dos corpos parentais.

Essa discussão avançou muito mais com o trabalho de Connolly *et al.* (1998), cujos dados associam os processos com os tipos texturais dos côndrulos. Para estes autores, as texturas condrícticas poderiam ser formadas como produtos de fusões incompletas (olivina porfirítica e microporfirítica) a completas (olivina barrada). Além disso, a temperatura máxima do aquecimento rápido alcançaria até  $2100^{\circ}\text{C}$  com um mínimo de  $1750^{\circ}\text{C}$  para formação dos côndrulos.

Em contraponto, Alexander *et al.* (2008), apresentam dados que discordam da temperatura proposta por Connolly *et al.* (1998). De acordo com estes autores, a temperatura de formação dos côndrulos variaria entre  $1973$  e  $2273^{\circ}\text{C}$ , assim como também demonstram que, durante o processo de fusão, os côndrulos funcionam essencialmente como um sistema fechado, pelo menos para os elementos com volatilidade igual ou menor que a do sódio (Na).

Palme *et al.* (2015) ressaltam que apesar dos côndrulos serem os elementos de maior destaque no estudo dos meteoritos não diferenciados, não se deve desconsiderar as relações com a matriz. Uma vez que se infere que existe uma complementariedade entre as razões elementais de Si/Mg e Fe/Mg da matriz com os côndrulos.

Os côndrulos são assim relíquias dos processos que deram origem ao Sistema Solar. Conhecê-los e os compreender é aprender uma parte da nossa história. A melhor compreensão destes processos evolutivos nos estágios primitivos do Sistema Solar se torna possível mediante o estudo das texturas e composições dos minerais presentes em cada um deles. Todavia, é primordial entender que, apesar de em um condrito existirem muitos côndrulos, cada um deles com uma composição diferente e, provavelmente, os mecanismos que incorreram na sua formação podem ter ocorrido em momentos e de formas significativamente distintas, ou seja, cada côndrulo é representante de um momento singular nesta história.

## **Referências**

- ALEXANDER, C.M.O'D.; GROSSMAN, J.N.; EBEL, D.S.; CIESLA, F.J. The formation conditions of chondrules and chondrites. *Science*, [s. l.], v. 320, p. 1617-1619, 2008.
- BREARLEY, A.J. Nebular versus Parent-body Processing. In: HOLLAND, H.D.; TUREKIAN, K.K. *Meteorites, Comets and Planets: Treatise on Geochemistry*. [S. l.]: Elsevier, 205. v. 1, cap. 109, p. 143-200. ISBN 0080447201.
- CONNOLLY, H.C.; JONES, B.D.; HEWINS, R.H. The flash melting of chondrules: an experimental investigation into the melting history and physical nature of chondrule precursors. *Geochimica et Cosmochimica Acta*, [s. l.], v. 62, ed. 15, p. 2725-2735, 1998. [https://doi.org/10.1016/S0016-7037\(98\)00176-8](https://doi.org/10.1016/S0016-7037(98)00176-8)
- ENGRAND, C. Meteorites and cosmic dust: Interstellar heritage and nebular processes in the early Solar System. *EPJ Web of Conferences*, [S. l.], v. 18, n. 05001, p. 1-26, 27 jan. 2012. <https://doi.org/10.1051/epjconf/20111805001>
- GOODING, J.L.; KEIL, K. Relative abundances of chondrule primary textural types in ordinary chondrites and their bearing on conditions of chondrule formation. *Meteoritics*, [s. l.], v. 16, ed. 1, p. 17-43, 1981. <https://doi.org/10.1111/j.1945-5100.1981.tb00183.x>
- HEWINS, R.H. Experimental studies of chondrules. *Meteorites and the early solar system*, [s. l.], p. 660-679, 1988.
- HEWINS, R.H. Chondrules. *Annual Review of Earth and Planetary Sciences*, [s. l.], v. 25, p. 61-87, 1 maio 1997. <https://doi.org/10.1146/annurev.earth.25.1.61>
- HEWINS, R.; CONNOLLY, H.C.; LOFGREN, G.E.; LIBOUREL, G. Experimental Constraints on Chondrule Formation. *Chondrites and the Protoplanetary Disk*, [s. l.], v. 341, p. 286, 2005.
- JACQUET, E. Meteorite petrology versus genetics: Toward a unified binomial classification. *Meteoritics and Planetary Science*, [s. l.], v. 57, ed. 9, p. 1774-1794, 13 ago. 2022. <https://doi.org/10.1111/maps.13896>
- JONES, R.H. Petrology of FeO-poor, porphyritic pyroxene chondrules in the Semarkona chondrite. *Geochimica et Cosmochimica Acta*, [s. l.], v. 58, ed. 23, p. 5325-5340, 1994. [https://doi.org/10.1016/0016-7037\(94\)90316-6](https://doi.org/10.1016/0016-7037(94)90316-6)
- LODDERS, K. Solar System Abundances of the Elements. In: GOSWAMI, A.; REDDY, B. *Principles and Perspectives in Cosmochemistry: Astrophysics and Space Science*

- Proceedings. Berlin, Heidelberg: Springer, 2010. p. 379-417. ISBN 978-3-642-10351-3. E-book. [https://doi.org/10.1007/978-3-642-10352-0\\_8](https://doi.org/10.1007/978-3-642-10352-0_8)
- LOFGREN, G.E. A dynamic crystallization model for chondrule melts. International conference: Chondrules and the protoplanetary disk, [s. l.], p. 187-196, 1996.
- MCSWEEN, H.Y. Chemical and petrographic constraints on the origin of chondrules and inclusions in carbonaceous chondrites. *Geochimica et Cosmochimica Acta*, [s. l.], v. 41, ed. 12, p. 1843-1860, 1977. [https://doi.org/10.1016/0016-7037\(77\)90216-2](https://doi.org/10.1016/0016-7037(77)90216-2)
- MERRILL, G.P. On chondrules and chondritic structure in meteorites. *Nacional Academy of Sciences of the United States of America*, [s. l.], v. 6, ed. 8, p. 449-472, 1920.
- OLIVEIRA, H.M. Meteoritos: Introdução à meteorítica e uma visão dos meteoritos brasileiros. 3. ed. Rio de Janeiro: [s. n.], 2020. 114 p. ISBN 9786500046281.
- PALME, H.; HEZEL, D.C.; EBEL, D.S. The origin of chondrules: Constraints from matrix composition and matrix-chondrule complementarity. *Earth and Planetary Science Letters*, [S. l.], v. 411, p. 11-19, 1 fev. 2015. <https://doi.org/10.1016/j.epsl.2014.11.033>
- PALME, H.; ZIPFEL, J. The Chemistry of Solar System Materials: Sun, Planets, Asteroids, Meteorites and Dust. In: TRIGO-RODRÍGUEZ, J.; GRITSEVICH, M.; PALME, H. Assessment and Mitigation of Asteroid Impact Hazards. [S. l.]: Springer, Cham, 2017. v. 46, p. 33-53. ISBN 978-3-319-46179-3. Disponível em: [https://link.springer.com/chapter/10.1007/978-3-319-46179-3\\_3#citeas](https://link.springer.com/chapter/10.1007/978-3-319-46179-3_3#citeas). Acesso em: 6 fev. 2023.
- PAQUE, J.; BUNCH, T. Stardust to Planetesimals: A Chondrule Connection?. *ASP Conference Series*, [s. l.], v. 122, p. 253-269, 1 jan. 1997.
- SCOTT, E.R.D.; KROT, A.N. Chondrites and their Components. In: HOLLAND, H.D.; TUREKIAN, K.K. *Meteorites, Comets and Planets: Treatise on Geochemistry*. [S. l.]: Elsevier, 205. v. 1, cap. 107, p. 143-200. ISBN 0080447201.
- ZANDA, B. Chondrules. *Earth and Planetary Science Letters*, [s. l.], v. 224, p. 1-17, 30 jul. 2004. <https://doi.org/10.1016/j.epsl.2004.05.005>

## Instruções para publicação na Revista

### *Meteoritics & Planetary Science Submission Guidelines*

#### **Submission**

New submissions should be made via the Research Exchange [submission portal](#). You may check the status of your submission at any time by logging on to [submission.wiley.com](#) and clicking the “My Submissions” button. For technical help with the submission system, please review our [FAQs](#) or contact [submissionhelp@wiley.com](mailto:submissionhelp@wiley.com). If you still have problems, contact the editorial office.

Authors are responsible for providing keywords for their articles. You can choose keywords from the keywords list when submitting the manuscript. You will be able to add new keywords, if needed.

**MaPS Preprint Policy:** This journal will consider articles previously available as preprints on non-commercial servers and are subject to the usual review process; authors submitting articles previously available as preprints must disclose explanation for preprint posting upon time of submission to the journal. Authors are requested to update any pre-publication versions with a link to the final published article.

**For submissions started prior to April 3, 2023, please visit [Manuscript Central](#) to manage or complete your submission.**

#### **General**

Submitted articles are judged from the standpoint of scientific originality and appropriateness of the subject matter to the journal. Categories of papers to be considered are: *Invited Reviews, Articles, Reports, and Critical comments*.

*Invited reviews* are solicited by the Editor on the advice of the Editorial Board. Timely and important papers in all categories can be handled in an expedited fashion. When preparing such a manuscript, authors should consult with the Editors as early as possible. The final decision on all submitted papers rests with the Editor.

*Articles* are original papers that pertain to broad areas of interest to the scientific community. They should be as concise as possible and should not exceed 16 manuscript s. Longer papers need to be discussed with the Editor before submission. If the published version of your paper exceeds, we will assess a charge of \$70 for each additional page. These charges will be billed with reprints and color orders.

*Reports* are papers which, while of high quality and importance, are primarily of interest to specialists. They contain subject matter that deals with a single but significant detail of topic of interest to the readers.

*Critical comments* on a previously published paper are encouraged, provided such comments are constructive. They should be submitted within 12 months of publication of the original article. The author of the original paper will be given the opportunity to prepare a *Reply*.

Submission of a manuscript is understood to imply that both the whole and parts of the paper are original, unpublished and not being considered elsewhere. By submitting a manuscript, the author(s) agrees that the copyright of the paper will be transferred to the Meteoritical Society upon publication, except in cases where the author(s) works for an organization that does not permit such assignment.

## **Review Process**

A submitted paper is forwarded to the Editor who then passes it to an Associate Editor in the subject area. If appropriate, the Associate Editor will identify external reviewers. The Associate Editor and the reviewers may recommend to the Editor that the paper be:

- accepted for publication,
- accepted after revision and further review,
- rejected.

The review process ensures that accepted papers are of the highest quality possible and that they are well presented. Authors are expected to acknowledge the contribution of the reviewers, whether the reviewers are anonymous or known to the authors. The final version should be submitted within 6 months for final evaluation. Papers that are not revised within 6 months will be treated as new submissions and will be sent for

review.

## Data Sharing and Data Accessibility

*Please review Wiley's policy [here](#). This journal expects data sharing.*

*Meteoritics and Planetary Science* recognizes the many benefits of archiving research data. *MaPS* expects you to archive all the data from which your published results are derived in a public repository. The repository that you choose should offer you guaranteed preservation (see the registry of research data repositories at <https://www.re3data.org/>) and should help you make it findable, accessible, interoperable, and re-useable, according to FAIR Data Principles (<https://www.force11.org/group/fairgroup/fairprinciples>). All accepted manuscripts are required to publish a data availability statement to confirm the presence or absence of shared data. If you have shared data, this statement will describe how the data can be accessed, and include a persistent identifier (e.g., a DOI for the data, or an accession number) from the repository where you shared the data. Authors will be required to confirm adherence to the policy. If you cannot share the data described in your manuscript, for example for legal or ethical reasons, or do not intend to share the data then you must provide the appropriate data availability statement. *MaPS* notes that FAIR data sharing allows for access to shared data under restrictions (e.g., to protect confidential or proprietary information) but notes that the FAIR principles encourage you to share data in ways that are as open as possible (but that can be as closed as necessary).

Sample statements are available [here](#). If published, all statements will be placed in the heading of your manuscript.

## Page and Color Charges

*Meteoritics & Planetary Science* encourages authors to submit papers that do not exceed 16 printed pages. The journal assesses a charge of \$70 per page for each printed page over 16 pages (i.e. if your printed version is 23 pages long, you will be charged \$70 per page for pages 17-23). A page charge form will be sent to all authors with page proofs and must be returned prior to publication. Longer papers and reviews should be discussed with the Editor before submission.

The rate for color charges is \$350 per printed page. There is no fee for color illustrations published online.

**Please note: if Open Access is selected, the standard publication fees will be waived; however, if you opt to print figures in color, color charges apply. There are no additional charges if figures are printed in black and white.**

### **Style**

For details on manuscript form and style, refer to the following and to a recent issue of *Meteoritics and Planetary Science* as well as the Chicago Manual of Style.

For review, submit a full electronic copy (the text, all tables, and all figures) of your manuscript. The final text of your manuscript should be prepared using Microsoft Word and the tables should be prepared with Excel or using a table format in your word processor so that we can easily typeset them.

*MaPS* now accepts LaTeX files but only for production purposes. Please only provide LaTeX files if your manuscript has been accepted and is in its final version; however, the PDF or Word files of the complete article and all related files still need to be submitted in the first instance.

Your manuscript must be written in English and should include a title, author(s)' name(s), their full mailing addresses, affiliations, corresponding author's e-mail address, an abstract, main text, acknowledgments, references, tables, figures, and figure captions. Use a single spaced, one-column page format, and avoid footnotes.

Abstract is mandatory. Take great care in writing your abstract. It often determines whether the paper will be read in depth; also, your abstract will appear unaccompanied by the main text in invitation e-mails sent to potential reviewers. Abstracts should not exceed 200 words.

### **Preparation of Manuscripts**

Make the text clear, concise, and accurate. The text should reflect American spelling.

Place acknowledgments at the end of the text before the References section.

Use the International System of Units (SI) for quantities and units unless a strong case can be made otherwise.

Mark clearly the subheadings within the various sections.

New meteorite names must be approved by the Meteorite Nomenclature Committee of the Meteoritical Society. For details, contact Dr. Michael Weisberg, Kingsborough College of the City University of New York (CUNY), Department of Physical Sciences, 2001 Oriental Blvd., Brooklyn, NY 11235, USA.

Existing meteorite names should conform to the spelling given in the Catalogue of meteorites (5th edition, 2000, Cambridge University Press) by M. M. Grady, or in subsequent issues of the Meteoritical Bulletin (available online or in the summer supplement to Meteoritics & Planetary Science). The full names of meteorites should be used in titles and at first mention in the text.

Abbreviations, including those published in the Antarctic Meteorite Newsletter and the Meteoritical Bulletin, may be used in tables and elsewhere. Note, that in the abbreviated form, there should be a space between the place name and the number. In addition, names of Antarctic meteorites recovered prior to 1981 may have an A in place of the space. Japanese meteorites (e.g. Yamato, Asuka) should have a dash between the name and the number and also between the abbreviation ("Y" and "A") and the number (e.g. Y-793169). See the list of standard abbreviations and examples of their proper usage.

Whenever possible, use mineral names approved by the International Mineralogical Association (see Fleischer M., Mandarino J. A. 1995. Glossary of mineral species, 7th edition. Tucson, Arizona: Mineralogical Record). If you wish to introduce a new mineral name, or to redefine, discredit, or rename an existing mineral, refer to Mineralogy and Petrology 37:157–179 or the following issues of American Mineralogist 72:1031–1042; 73; 200.

## Preparation of Tables

The following guide is based on The Chicago Manual of Style (14th edition, University of Chicago Press, 1993). Examples are shown for the newer scientific style of citation recommended for natural sciences and social sciences (for details see p. 640–699). Submit electronic copies of your tables in Word format. You can send PDF versions of

your tables for review, but do not send the “camera-ready” tables or PDF versions when you submit the final copy for typesetting, we cannot use them to typeset your manuscript. Provide titles for all tables.

Follow MAPS style when preparing tables:

- Use n.d. (not detected) or similar notation rather than 0.0.
- Tables should have short titles. Relative clauses should be avoided. Details or explanation should appear as table footnotes.
- Title format is: “Table 1. The first word in the title is capitalized with the rest in lower case.” The title ends with a period and the caption is aligned left.
- Horizontal lines should separate the title, the table header, the body of table, and the footnotes.
- Only the first word in each cell of the table header should be capitalized.
- Footnotes, with or without superiors (which may be numbers, letters, or symbols) are aligned left and end with a period. There is no line space between footnotes.
- Vertical lines are not used to separate columns.
- Borders are not used around tables.

## Preparation of Illustrations

Halftone and color images should be scanned at 300 pixels per inch (ppi). Line art should be scanned at 1200 ppi. Use TIFF, PDF or EPS formats for submission of images and figures.

More detailed information on the submission of electronic artwork can be found at <http://authorservices.wiley.com/bauthor/faq.asp>.

Each figure should be submitted as a separate file, but arrange multiple-panel figures into one composite file.

Figures are often reduced in size when typesetting. Keep this in mind when sizing symbols and letters and do not make the figures larger than 7" x 7" (17.5 cm x 17.5 cm). Oversized and difficult to handle figures should be discussed with the editorial office before submission.

Line drawings, if possible, should fit in a single column (width 3.4" or 9 cm). Place all figure captions at the end of the manuscript. Here is an example of a figure caption:

*Fig. 1. Trapped heavy noble gases in enstatite chondrites.*

Within the text, figures (whether line drawings or photographs) are referred to in the abbreviated form as, for example, Fig. 1.

## Preparation of References

*Meteoritics & Planetary Science* follows *Chicago Manual of Style* reference style. The journal discourages the citation of abstracts and material that have not been referenced.

References that are in the process of publication will be referred to as "Forthcoming." For example:

Smith A. B. Forthcoming. Marvin: A new martian meteorite from the Moon. *Journal of*

...

List references at the end of each paper in alphabetical and chronological order and cross-check the reference list with the text.

When listing several papers by the same author (some of which have several authors) use this sequence:

**One author:** chronological order:

French, B. M. 1967. Sudbury Structure, Ontario: Some Petrographic Evidence for Origin by Meteorite Impact. *Science* **156**: 1094– 8.

French, B. M. 1968. Sudbury Structure, Ontario: Some Petrographic Evidence for an Origin by Meteorite Impact. In *Shock Metamorphism of Natural Materials*, edited by B. M. French and N. M. Short, 383– 412. Baltimore, MD: Mono Book Corp.

**Two or more authors:** alphabetical then chronological:  
Prasad, M. S., and Khedekar, V. D. 2003. Impact Microcrater Morphology on Australasian Microtectites. *Meteoritics & Planetary Science* **38**: 1351– 71.

Prasad, M. S., and Sudhakar, M. 1998. Microimpact Phenomena on Australasian Microtectites: Implications for Ejecta Plume Characteristics and Lunar Surface Process. *Meteoritics & Planetary Sciences* **33**: 1271– 9.

Prasad, M. S., Gupta, S. M., and Kodagali, V. N. 2003. Two Layers of Australasian Impact Ejecta in the Indian Ocean? *Meteoritics & Planetary Sciences* **38**: 1373– 81.

Use the following style to format references:

**Journal:**

Keng, Shao-Hsun, Chun-Hung Lin, and Peter F. Orazem. 2017. "Expanding College Access in Taiwan, 1978–2014: Effects on Graduate Quality and Income Inequality." *Journal of Human Capital* 11(1, Spring): 1–34. <https://doi.org/10.1086/690235>.

*Note:* CMS allows either use first names or initials, but it should be consistent throughout the reference list.

**Book:**

Purkis, Samuel, and Victor Klemas. 2011. *Remote Sensing and Global Environmental Change*. Oxford: Wiley-Blackwell

**Chapter in a book:**

Messing, Charles G., John K. Reed, Sandra D. Brooke, and Steve W. Ross. 2008. "Deep-Water Coral Reefs of the United States." In *Coral Reefs of the USA*, edited by Bernhard M. Riegl and Richard E. Dodge, 767–92. Dordrecht: Springer.

**Abstract:**

Keng, Shao-Hsun, Chun-Hung Lin, and Peter F. Orazem. 2017. "Expanding College Access in Taiwan, 1978–2014: Effects on Graduate Quality and Income Inequality" (abstract). *Journal of Human Capital* 11(1, Spring): 1–34. <https://doi.org/10.1086/690235>

**LPSC:**

Reference should include author, title, LPSC number, and abstract.

Tonui, E. K., Zolensky, M. E., Hiroi, T., Lipschutz, M. E., and Okudaira, K. 2002. Petrographic, Chemical, and Spectroscopic Data on Thermally Metamorphosed Carbonaceous Dhondrites. *23rd Lunar and Planetary Science Conference*, abstract

**MetSoc abstracts published in print and online:**

Newton J., Franchi I. A., and Pillinger C. T. 2000. The oxygen-isotopic record in enstatite meteorites (abstract #5466). *Meteoritics & Planetary Science* 35:A688.

**For online only MetSoc Abstracts:**

Newton J., Franchi I. A., and Pillinger C. T. 2012. The oxygen-isotopic record in enstatite meteorites (abstract). *Meteoritics & Planetary Science* 47 (Suppl.):5443.pdf.

**Conference proceedings:**

Chiswick, Bake R. 1977. "A Longitudinal Analysis of the Occupational Mobility of Immigrants." In *Proceedings of the 30th Annual Winter Meetings, Industrial Relations Research Association*, ed. Barbara D. Dennis, 20–7 Madison, WI: IRRA.

**Thesis:**

Pruzinsky, Nina. 2018. "Identification and Spatiotemporal Dynamics of Tuna (Family: Scombridae; Tribe: Thunnini) Early Life Stages in the Oceanic Gulf of Mexico." MS thesis, Nova Southeastern University. [https://nsuworks.nova.edu/occ\\_stuetd/472/](https://nsuworks.nova.edu/occ_stuetd/472/).

Additional reference notes:

- In the text, two or more authors should be listed as first author's last name followed by "et al."
- Use full titles and journal names.
- When referring to material published on the Internet, provide the following information: author/editor, title of page, date that you accessed the source, cite the address (URL) accurately (include the access mode http, ftp, telnet, etc.).
- A press release should be referenced as an unpublished document:

National Transportation Safety Board, "Airline fatalities for 1994 climbed to five-year high," news release, January 17, 2004.

**Supporting Information**

Material that is supplementary to the printed text of an article (eg video clips, extra images, tables, etc.) can be hosted online with the journal at the discretion of the Editor. Authors are required to provide a legend (include with your figure legends) explaining what is contained in the supplementary file. Specific author guidelines for submitting this material to the editorial office and production can be found at: <http://authorservices.wiley.com/bauthor/suppmat.asp>.

## **Page Proofs**

Proofs are sent directly to the corresponding author from Wiley. The author is responsible for reviewing the proofs in the online proofing system. Please read the proof(s) and submit the file to the typesetter within 48 hours of receipt. If you require more time to review the proofs, please contact the production editor.

## **Author Services**

Author Services enables authors to track their article -- once it has been accepted -- through the production process to publication online and in print. Authors can check the status of their articles online and choose to receive automated e-mails at key stages of production so they don't need to contact the production editor to check on progress. Visit <http://authorservices.wiley.com/> for more details on online production tracking and for a wealth of resources including FAQs and tips on article preparation, submission, and more.

Prior to submitting your manuscript, consider visiting the Author Service resource [here](#) for tips on best practices on how to make your search engine friendly and more discoverable. You can also view this helpful [PDF guide](#) on how authors can improve Search Engine Optimization for their articles.

## **Author Name Change Policy**

In cases where authors wish to change their name following publication, Wiley will update and republish the paper and redeliver the updated metadata to indexing services. Our editorial and production teams will use discretion in recognizing that name changes may be of a sensitive and private nature for various reasons including (but not limited to) alignment with gender identity, or as a result of marriage, divorce, or religious

conversion. Accordingly, to protect the author's privacy, we will not publish a correction notice to the paper, and we will not notify co-authors of the change. Authors should contact the journal's Editorial Office with their name change request.

## **Correction to Authorship Form**

In accordance with [Wiley's Best Practice Guidelines on Research Integrity and Publishing Ethics](#) and the [Committee on Publication Ethics' guidance](#), MAPS will allow authors to correct authorship on a submitted, accepted, or published article if a valid reason exists to do so. All authors – including those to be added or removed – must agree to any proposed change. To request a change to the author list, please complete the [Request for Changes to a Journal Article Author List Form](#) and contact either the journal's editorial or production office, depending on the status of the article. Authorship changes will not be considered without a fully completed Author Change form. [Correcting the authorship is different from changing an author's name; the relevant policy for that can be found in [Wiley's Best Practice Guidelines](#) under "Author name changes after publication."]

## **Compliance with Coalition S**

This journal offers a number of license options for published papers; information about this is available here: <https://authorservices.wiley.com/author-resources/Journal-Authors/licensing/index.html>. The submitting author has confirmed that all co-authors have the necessary rights to grant in the submission, including in light of each co-author's funder policies. If any author's funder has a policy that restricts which kinds of license they can sign, for example if the funder is a member of [Coalition S](#), please make sure the submitting author is aware.

## **Wiley Editing Services**

Wiley provides authors with a suite of editing services ranging from manuscript preparation to article promotion. See below for a full list of services, and for more information, see the [Wiley Editing Services site](#).

Article Preparation Services – helping authors prepare their articles, allowing them to submit with confidence, improve their chances of acceptance, and save valuable research time.

- English Language Editing
- Academic Translation
- Figure Formatting
- Journal Recommendation
- Manuscript Formatting
- Academic Illustration
- Graphical Abstract Design

Article Promotion Services – professional video, design, and writing services to help authors extend their reach and maximize the impact of their research.

- Video Creation
- Conference Poster Creation
- Cover Image Design
- Infographic Creation
- Lay Summaries
- Research News Stories

### **Reprints/Offprints**

An electronic PDF version of the final article is provided through Author Services upon publication; a link to order hardcopy reprint order form is included with proofs.

### **Refer and Transfer Program**

Wiley believes that no valuable research should go unshared. This journal participates in Wiley's Refer & Transfer program. If your manuscript is not accepted, you may receive a recommendation to transfer your manuscript to another suitable Wiley journal, either through a referral from the journal's editor or through our Transfer Desk Assistant.

### **Note to NIH Grantees**

Pursuant to NIH mandate, Wiley-Blackwell will post the accepted version of contributions authored by NIH grant-holders to PubMed Central upon acceptance, if the

author acknowledges NIH in the 'Acknowledgement' section of the paper. This accepted version will be made publicly available 12 months after publication. For more information on the NIH mandate: <http://authorservices.wiley.com/bauthor/CTA.asp>

## **Open Access Option**

Open Access is available to authors of primary research articles who wish to make their article available to non-subscribers on publication, or whose funding agency requires grantees to archive the final version of their article. With Open Access, the author, the author's funding agency, or the author's institution pays a fee to ensure that the article is made available to non-subscribers upon publication via Wiley Online Library, as well as deposited in the funding agency's preferred archive. For more information about Article Publication Charges, please visit the [Open Access page](#).

Any authors wishing to send their paper Open Access will be required to complete the payment form available from our website at: [https://authorservices.wiley.com/bauthor/onlineopen\\_order.asp](https://authorservices.wiley.com/bauthor/onlineopen_order.asp) Prior to acceptance there is no requirement to inform an Editorial Office that you intend to publish your paper Open Access if you do not wish to. All Open Access articles are treated in the same way as any other article. They go through the journal's standard peer-review process and will be accepted or rejected based on their own merit.

If your paper is accepted, the author identified as the formal corresponding author for the paper will receive an email prompting them to login into Author Services; where via the Wiley Author Licensing Service (WALS) they will be able to complete the license agreement on behalf of all authors on the paper. For authors signing the copyright transfer agreement If the Open Access option is not selected the corresponding author will be presented with the copyright transfer agreement (CTA) to sign. The terms and conditions of the CTA can be previewed in the samples associated with the Copyright FAQs below: CTA Terms and Conditions [http://authorservices.wiley.com/bauthor/faqs\\_copyright.asp](http://authorservices.wiley.com/bauthor/faqs_copyright.asp) For authors choosing Open Access, if the option is selected the corresponding author will have a choice of the following Creative Commons License Open Access Agreements (OAA): Creative Commons Attribution License OAA Creative Commons Attribution Non-Commercial License OAA Creative Commons Attribution Non-Commercial - NoDerivs License OAA To preview the terms and conditions of these open access agreements please visit the Copyright FAQs hosted on Wiley Author Services

[http://authorservices.wiley.com/bauthor/faqs\\_copyright.asp](http://authorservices.wiley.com/bauthor/faqs_copyright.asp) and visit  
<http://www.wileyopenaccess.com/details/content/12f25db4c87/Copyright--License.html>. If you select the Open Access option and your research is funded by The Wellcome Trust and members of the Research Councils UK (RCUK) you will be given the opportunity to publish your article under a CC-BY license supporting you in complying with Wellcome Trust and Research Councils UK requirements. For more information on this policy and the Journal's compliant self-archiving policy please visit: <http://www.wiley.com/go/funderstatement>.



Cristine Pereira <cristinepereira1@gmail.com>

---

## Meteoritics & Planetary Science-MS MAPS-4068

2 mensagens

---

Agnieszka Baier <onbehalfof@manuscriptcentral.com>

Responder a: baiera@arizona.edu

Para: cristinepereira1@gmail.com

11 de fevereiro de 2024 às 21:44

This is an automated message sent by the MAPS Online Review and Submission System.

11-Feb-2024

Dear Miss Pereira,

Your manuscript, entitled "Unraveling the Origins of the Solar System: A Comprehensive Petrological Investigation of Chondrules within the Campos Sales Meteorite," has been successfully submitted and is being considered for publication in Meteoritics & Planetary Science.

Your manuscript ID is MAPS-4068.

Please, mention the above manuscript ID in all future correspondence or when calling the editorial office with questions.

Our journal is currently transitioning to Wiley's Research Exchange submission portal. If you submitted this manuscript through our Research Exchange site, you can view the status of your manuscript by logging into the submission site at [wiley.atyponrex.com/journal/MAPS](https://wiley.atyponrex.com/journal/MAPS).

If you submitted this manuscript through ScholarOne, you can view the status of your manuscript by checking your Author Center after logging in to <https://mc.manuscriptcentral.com/maps>

In the next few days, the editorial office will check the submitted files and the paper will be forwarded to an associate editor. If you have any question about the paper while it's in review, please contact the MAPS office.

This journal offers a number of license options for published papers; information about this is available here: <https://authorservices.wiley.com/author-resources/Journal-Authors/licensing/index.html>. The submitting author has confirmed that all co-authors have the necessary rights to grant in the submission, including in light of each co-author's funder policies. If any author's funder has a policy that restricts which kinds of license they can sign, for example if the funder is a member of Coalition S, please make sure the submitting author is aware.

Thank you for submitting your manuscript to Meteoritics & Planetary Science.

Sincerely,  
Meteoritics & Planetary Science Editorial Office

---

Cristine Pereira <cristinepereira1@gmail.com>

Para: Débora Rios <dcrios2016@gmail.com>, Debora Correia Rios <dcrios@ufba.br>

12 de fevereiro de 2024 às 15:03

**Cristine de Almeida Pereira**

[Texto das mensagens anteriores oculto]

**METEORITICS  
& PLANETARY SCIENCE**

JOURNAL HOME

AUTHOR GUIDELINES

EDITORIAL CONTACT

## Submission Overview

**Initial Submission**

This manuscript has been submitted to the editorial office for review. Changes cannot be made during editorial review, but you can view the information and files you submitted, below.

Article Type	Article		
Title	Unraveling the Origins of the Solar System: A Comprehensive Petrological Investigation of Chondrules within the Campos Sales Meteorite		
Manuscript Files	Name	Type of File	Size
	<a href="#">2024 Feb7 Pereira et al Campos Sales.docx</a>	Main Document - MS Word	3.7 MB
	<a href="#">2024 Feb 7 Pereira et al Campos Sales cover letter DCR.docx</a>	Cover letter / Comments	14.6 KB
	<a href="#">2024 Feb 7 Pereira et al Campos Sales Conflict of Interest.pdf</a>	Conflict of Interest	86.8 KB
Abstract	This paper investigates chondrules, integral components of chondritic meteorites from the early Solar System. Focusing on 33 chondrules from the Campos Sales Meteorite, an L5		

ordinary chondrite, we explore their compositions, mineral formation, and origin. Considering the hypothesis that chondrules may be "magmatic" droplets, we examine the compositions of these "primitive melts." Campo Sales' chondrules, mostly circular with some undefined shapes, contain olivine, enstatite, augite, chromite, troilite, Cl-apatite, and silicon dioxide. Varied textures, including barred, radial, and granular patterns, alongside skeletal crystals of olivine, enstatite, and augite, are observed, some featuring intergrowth textures. Chemical data reveal compositional homogeneity, indicating a chemical reequilibration event. Despite challenges in discerning elemental patterns, the study underscores rapid crystallization and preservation of skeletal shapes and volatile elements, suggesting accretion before complete solidification. These findings offer insights into early Solar System evolution, emphasizing chondrules as records of magmatic processes amid challenges in understanding their elemental patterns. The study provides comprehensive insights into type L chondrules, unraveling their composition, formation, and the intricate processes shaping the early Solar System.

## Authors

	Name	Email	Country/Location
Cristine de Almeida Pereira <sup>1, 2</sup> Corresponding Author	cristinepereira1@gmail.com		Brazil
 <a href="#">0000-0003- 3385-1322</a>			
Herbet Conceição <sup>1</sup>	herbet@academico.ufs.br		Brazil
Débora Correia Rios <sup>2, 3</sup>	dcrios2016@gmail.com		Canada

## Affiliations

We will use the best match from our database to determine if your manuscript is eligible for special benefits. Matched organizations are for

1. Universidade Federal de Sergipe. Instituto de Geociências. Programa de Pós-Graduação em Geociências e Análises de Bacias, Complexo Laboratorial Multusuário. Avenida Marechal Rondon, s/n, Jardim Rosa Elze, São Cristóvão. 49.100-000, Aracaju, Sergipe – Brasil  
**Matched organization**

internal purposes and will  
not be published.

Universidade Federal de Sergipe  
SÃO CRISTÓVÃO, Brazil

2. Universidade Federal da Bahia. Instituto de Geociências. Geologar – Ciências da Terra para a Sociedade, Laboratório de Petrologia Aplicada a Pesquisa Mineral. Programa de Pós-Graduação em Geologia. Rua Barão de Jeremoabo, s/n, Campus Universitário de Ondina. 40.170-290, Salvador, Bahia – Brasil

**Matched organization**

Universidade Federal da Bahia Instituto de Geociencias  
SALVADOR, Brazil

3. Western Ontario University, Zircon and Accessory Phases Laboratory – ZAPLab, Department of Earth Sciences, University of Western Ontario. 1151, Richmond St. N., London, Ontario, N6A 5B7, Canada

**Matched organization**

Western University Faculty of Science  
LONDON, Canada

## Additional Information

### Funders

No funding was received for this manuscript

### Keywords

Chondrules; Campo Sales Meteorite; Solar System Formation; Origins Processes

### Keyword List

- Chondrule(s)
- Petrography
- Petrology

### Meteorite Name

Yes

### Is this submission for a special issue?

No, this is not for a special issue

Has this manuscript been submitted previously to this journal?

No, it wasn't submitted previously

#### Suggested Reviewers

Amanda Tosi

amandatosi@hotmail.com

Universidade Federal do Rio de Janeiro

Giampaolo Sighinolfi

sighinolfig@yahoo.it

This reviewer has no Affiliation

#### Opposed Reviewers

*No response provided*

#### Cover letter / Comments

Yes, I'd like to add a cover letter or comments

(see [Manuscript Files](#))

#### Preferred Editors

Gordon Osinski

#### History

Submitted On 7 February 2024 by Cristine Pereira

› [Show this version history](#)

Submission Started 7 February 2024 by Cristine Pereira



Pesquisar e-mail



Escrever



Traduza para o português

**Caixa de entrada**

Adiados

Importante

Enviados

Rascunhos

Mais

Dear Cristine Pereira,

Your manuscript "Unraveling the Origins of the Solar System: A Comprehensive Petrological Investigation of Chondrules within the Campos Sales Meteorite" has been successfully submitted and is being delivered to the Editorial Office of *Meteoritics & Planetary Science* for consideration.

You will receive a follow-up email with further instructions from the journal editorial office, typically within one business day. That message will confirm that the editorial office has received your submission and will provide your manuscript ID.

Thank you for submitting your manuscript to *Meteoritics & Planetary Science*.

Sincerely,

The Editorial Staff at *Meteoritics & Planetary Science*

**Marcadores**

[Imap]/Trash

Pessoal

Trabalho

Mais

By submitting a manuscript to or reviewing for this publication, your name, email address, and affiliation, and other contact details the publication might require, will be used for the regular operations of the publication, including, when necessary, sharing with the publisher (Wiley) and partners for production and publication. The publication and the publisher recognize the importance of protecting the personal information collected from users in the operation of these services and have practices in place to ensure that steps are taken to maintain the security, integrity, and privacy of the personal data collected and processed. You can learn more by reading our [data protection policy](#). In case you don't want to be contacted by this publication again, please send an email to [baiera@arizona.edu](mailto:baiera@arizona.edu).

Tabela 5.1 Dados químicos obtidos a partir das análises de cristais de olivina presentes no meteorito Campos Sales. Dados da fórmula estrutural obtidos a partir do cálculo para 4 átomos de oxigênio. Fo= Forsterita, Fa= Fayalita, Mo=Monticellita. C = centro, b = borda

Cristal	117	131	28	29	47	48	20	23	34	57	66	43	139	52	90	91	1	106
Posição	c	b	c	c	c	b	c	b	b	b	c	c	c	c	c	c	c	c
SiO <sub>2</sub>	38,33	38,99	38,61	38,71	38,98	38,66	39,11	39,32	38,95	38,15	38,96	39,42	39,2	37,99	37,87	37,77	38,13	37,73
TiO <sub>2</sub>	0,11		0,1	0,07			0,02			0,07	0,07	0,04		0,03				
Al <sub>2</sub> O <sub>3</sub>	1,72	0,36	0,05						0,09		0,18	0,31		0,09		0,52	0,01	
Cr <sub>2</sub> O <sub>3</sub>	0,11		0,08		0,04	0,08			0,04		0,05		0,07	0,13	0,05	0,13	0,08	0,08
FeO	20,72	20,97	21,23	20,86	21,7	21,48	21,45	20,3	20,82	21,96	20,68	19,66	19,04	21,99	22,02	22,01	22,04	22,52
MnO	0,47	0,46	0,44	0,55	0,4	0,44	0,48	0,41	0,53	0,58	0,42	0,35	0,36	0,39	0,46	0,44	0,39	0,43
MgO	38,39	38,74	39,44	39,8	38,84	39,21	38,9	39,65	39,52	38,93	39,11	40,33	41,04	39,52	39,47	39,11	39,31	39,11
CaO	0,14	0,08	0,04			0,04	0,04	0,06		0,03	0,09	0,04	0,06	0,01	0,01	0,03		0,06
Na <sub>2</sub> O		0,01															0,05	
K <sub>2</sub> O		0,06	0,02								0,07	0,04	0,03			0,02	0,01	
Total	99,99	99,67	100,01	99,99	99,96	99,91	100	99,87	99,82	99,95	99,71	99,95	99,95	99,98	99,96	99,98	99,98	99,94
Si	0,994	1,011	1,001	1,003	1,010	1,002	1,014	1,019	1,010	0,989	1,010	1,022	1,016	0,985	0,982	0,979	0,988	0,978
Al	0,053	0,011	0,002					0,003		0,005	0,009		0,003				0,016	
Fe	0,449	0,455	0,460	0,452	0,470	0,466	0,465	0,440	0,451	0,476	0,448	0,426	0,413	0,477	0,477	0,477	0,478	0,488
Mg	1,484	1,497	1,524	1,538	1,501	1,515	1,503	1,532	1,527	1,504	1,511	1,558	1,586	1,527	1,525	1,511	1,519	1,511
Total cations	2,998	2,992	3,001	3,007	2,992	2,997	2,994	3,008	3,004	2,992	2,999	3,019	3,031	2,999	2,998	2,996	2,996	2,991
End members																		
Fo	76,106	75,996	76,320	76,815	75,747	75,948	75,928	77,151	76,587	75,378	76,396	78,051	78,833	75,825	75,650	75,534	75,667	75,088
Fa	23,039	23,073	23,042	22,582	23,737	23,336	23,483	22,155	22,631	23,849	22,658	21,341	20,514	23,665	23,672	23,843	23,795	24,251
Mo	0,199	0,113	0,056	0,000	0,000	0,056	0,056	0,084	0,000	0,042	0,126	0,056	0,083	0,014	0,014	0,042	0,000	0,083

Tabela 5.2 Dados químicos obtidos a partir das análises de cristais de enstatita presentes no meteorito Campos Sales. Dados da fórmula estrutural obtidos a partir do cálculo para 3 átomos de oxigênio. En= Enstatita, Fs= Ferrossilita, Wo= Wolastonita. C = centro, b = borda

Cristal Posição	111 c	70 b	82 c	106 c	27 c	30 c	34 c	36 c	4 c	15 c	20 c	101 c	104 c	127 c	128 c	130 c	131 c	1 c	5 c	6 b
SiO <sub>2</sub>	55,7	55,5	55,9	55,5	56,0	55,7	55,9	55,9	56,0	56,1	56,0	55,8	56,0	56,2	56,2	55,9	56,3	56,5	56,5	56,1
FeO	13,3	13,0	13,2	12,7	13,2	13,6	13,1	13,3	13,3	13,1	12,7	12,8	12,4	12,0	11,7	11,5	10,9	11,2	11,1	11,2
MnO	0,5	0,5	0,5	0,5	0,5	0,4	0,5	0,6	0,6	0,5	0,5	0,4	0,4	0,4	0,4	0,3	0,3	0,3	0,5	0,3
MgO	28,3	29,4	29,3	29,4	29,4	28,9	29,7	29,2	29,3	29,4	29,9	29,4	29,9	30,3	30,4	30,3	31,1	30,9	30,8	30,5
CaO	0,6	0,6	0,8	0,8	0,5	0,6	0,5	0,7	0,5	0,7	0,6	0,9	0,9	0,7	0,8	0,8	0,7	0,6	0,8	0,8
Total	99,9	99,9	100,0	100,0	100,0	99,9	100,0	100,0	99,9	100,0	99,9	99,9	100,0	100,0	100,0	99,9	100,0	99,9	99,9	99,8
Si	1,988	1,982	1,994	1,979	1,996	1,993	1,992	1,993	1,998	1,998	1,994	1,987	1,991	1,991	1,989	1,978	1,987	1,994	1,996	1,988
Fe <sup>++</sup>	0,398	0,388	0,394	0,379	0,393	0,407	0,389	0,398	0,397	0,392	0,377	0,380	0,368	0,354	0,346	0,341	0,323	0,331	0,327	0,333
Mn	0,014	0,015	0,015	0,014	0,016	0,012	0,014	0,017	0,017	0,016	0,014	0,013	0,011	0,011	0,013	0,010	0,010	0,009	0,016	0,010
Mg	1,506	1,564	1,560	1,564	1,562	1,540	1,577	1,554	1,561	1,563	1,587	1,560	1,584	1,602	1,604	1,599	1,633	1,629	1,623	1,612
Ca	0,021	0,024	0,030	0,032	0,020	0,024	0,017	0,027	0,018	0,025	0,024	0,034	0,034	0,027	0,028	0,030	0,026	0,021	0,028	0,032
Total	3,999	3,998	3,999	3,999	3,997	3,998	4,000	4,000	3,998	3,999	4,001	4,000	4,000	4,000	3,998	4,000	4,001	3,998	3,997	4,001
En	0,78	0,79	0,79	0,79	0,79	0,78	0,80	0,79	0,79	0,79	0,80	0,79	0,80	0,81	0,81	0,81	0,83	0,82	0,82	0,82
Fs	0,21	0,19	0,20	0,19	0,20	0,21	0,20	0,20	0,20	0,20	0,19	0,19	0,18	0,18	0,18	0,17	0,16	0,17	0,17	0,17
Wo	0,01	0,01	0,02	0,02	0,01	0,01	0,01	0,01	0,01	0,01	0,01	0,02	0,02	0,01	0,01	0,02	0,01	0,01	0,01	0,02

Tabela 5.3 Dados químicos obtidos a partir das análises de cristais de augita presentes no meteorito Campos Sales. Dados da fórmula estrutural obtidos a partir do cálculo para 3 átomos de oxigênio. En= Enstatita, Fs= Ferrossilita, Wo= Wolastonita. C = centro, b = borda

Cristal	67	68	69	74	79	93	98	99	41	86	61	6	8	28	29	31	16	49	55	70	71	92	94	99	37
Posição	c	c	c	c	c	b	c	c	c	c	c	c	c	c	c	c	c	c	c	c	c	c	c	c	c
SiO <sub>2</sub>	53,9	54,7	54,3	54,1	53,8	54,1	53,7	54,1	53,9	54,2	54,6	54,5	54,6	54,5	54,1	54,2	54,0	52,8	54,3	54,6	54,2	54,3	54,1	54,0	54,8
Cr <sub>2</sub> O <sub>3</sub>	0,8	0,8	0,9	1,1	0,9	1,0	0,6	0,8	1,2	1,0	0,6	0,7	0,7	0,7	0,9	0,9	0,8	2,6	0,7	0,5	0,6	0,9	0,9	0,5	0,5
FeO	5,1	5,5	4,9	5,1	5,0	4,7	5,2	5,0	4,8	5,2	5,2	4,7	4,8	4,8	5,3	5,2	4,9	5,1	3,8	3,9	4,1	4,5	4,7	3,8	5,2
MgO	16,7	17,7	17,2	17,2	16,3	17,3	17,3	16,8	17,2	17,0	19,0	17,6	17,2	17,4	16,8	16,4	17,8	14,5	17,7	17,3	17,4	17,4	17,1	15,4	18,1
CaO	21,0	19,4	20,6	20,7	21,9	20,9	20,7	21,4	20,8	20,6	18,5	20,7	20,7	20,7	21,0	21,4	20,8	18,5	22,1	22,2	22,0	21,0	21,5	21,0	19,7
Na <sub>2</sub> O	0,7	0,7	0,6	0,6	0,4	0,7	0,6	0,5	0,6	0,5	0,7	0,6	0,7	0,7	0,6	0,7	0,5	2,0	0,4	0,5	0,4	0,6	0,5	1,3	0,5
Total	99,5	99,9	99,9	99,8	99,8	99,8	99,7	99,5	99,9	100,0	99,9	100,0	100,0	100,0	99,8	100,0	100,0	99,9	99,9	100,0	99,9	99,9	100,0	99,9	99,8
Si	1,985	1,996	1,987	1,984	1,975	1,979	1,968	1,992	1,973	1,983	1,983	1,989	1,993	1,991	1,983	1,986	1,973	1,935	1,984	1,990	1,980	1,985	1,979	1,964	1,999
Fe <sup>++</sup>	0,158	0,168	0,151	0,156	0,153	0,142	0,160	0,153	0,147	0,158	0,157	0,143	0,145	0,148	0,162	0,158	0,149	0,157	0,117	0,119	0,124	0,137	0,143	0,115	0,158
Mg	0,915	0,963	0,940	0,941	0,894	0,945	0,946	0,923	0,936	0,930	1,027	0,955	0,938	0,948	0,917	0,895	0,970	0,789	0,959	0,941	0,948	0,946	0,933	0,834	0,983
Ca	0,828	0,757	0,808	0,813	0,862	0,819	0,812	0,842	0,816	0,807	0,721	0,810	0,808	0,809	0,824	0,840	0,813	0,726	0,865	0,867	0,862	0,823	0,842	0,818	0,769
Na	0,049	0,048	0,044	0,041	0,029	0,046	0,041	0,037	0,040	0,038	0,048	0,045	0,047	0,047	0,043	0,050	0,038	0,141	0,031	0,037	0,031	0,042	0,035	0,089	0,038
Total	4,002	3,997	3,998	4,000	3,996	4,001	4,007	4,002	4,000	3,994	4,003	4,001	3,995	4,001	4,000	4,001	4,007	4,003	4,005	4,001	4,003	3,999	4,000	3,990	3,995
En	0,48	0,51	0,49	0,49	0,47	0,50	0,50	0,48	0,49	0,49	0,54	0,50	0,49	0,50	0,48	0,47	0,51	0,47	0,50	0,49	0,49	0,50	0,49	0,47	0,52
Fs	0,08	0,10	0,08	0,08	0,09	0,07	0,07	0,07	0,08	0,09	0,08	0,07	0,08	0,07	0,08	0,08	0,06	0,09	0,05	0,06	0,06	0,07	0,07	0,07	0,08
Wo	0,44	0,40	0,42	0,43	0,45	0,43	0,43	0,44	0,43	0,42	0,38	0,43	0,43	0,43	0,43	0,44	0,43	0,44	0,45	0,45	0,45	0,43	0,44	0,46	0,40

Tabela 5.4 Dados químicos obtidos a partir das análises de cristais de plagioclásio presentes no meteorito Campos Sales. Dados da fórmula estrutural obtidos a partir do cálculo para 5 átomos de oxigênio. Or= Ortoclásio, Ab= Albita, An= Anortita. C = centro, b = borda

Espectro	14	15	16	17	56	57	59	33	37	38	40	41	15	55	56
Posição	b	c	c	c	c	c	c	c	c	c	c	c	c	c	c
SiO <sub>2</sub>	65,44	65,05	65,19	65,17	64,48	65,05	64,01	65,29	64,99	65,29	65,28	64,04	65,31	65,24	64,93
TiO <sub>2</sub>	0	0,07			0,06	0,08	0,01						0,05		0,12
Al <sub>2</sub> O <sub>3</sub>	21,22	21,45	21,4	21,27	20,54	21,29	20,95	21,17	21,27	21,12	20,99	21,11	18,86	21,29	21,33
FeO	0,75	0,43	0,66	0,63	1,39	0,73	1,39	0,66	0,96	0,75	0,56	1,38	1,56	0,78	0,74
CaO	1,87	2	1,95	2,02	2,02	2,08	2,15	1,93	2,04	1,99	1,74	2,14	2,07	2	2,22
Na <sub>2</sub> O	10,08	10,1	9,98	10,18	8,86	9,29	8,96	10,06	9,92	9,87	9,49	9,5	8,83	9,93	9,61
K <sub>2</sub> O	0,64	0,88	0,81	0,73	1,43	1,3	1,35	0,9	0,82	0,98	1,94	1	0,67	0,61	0,98
Total	100	100	99,99	100	99,83	99,88	99,47	100,01	100	100	100	99,17	99,82	99,85	99,95
Si	2,89	2,88	2,88	2,88	2,87	2,88	2,86	2,89	2,88	2,89	2,89	2,87	2,90	2,88	2,87
Al	1,10	1,12	1,11	1,11	1,08	1,11	1,10	1,10	1,11	1,10	1,10	1,11	0,99	1,11	1,11
Total	3,99	3,99	4,00	3,99	3,95	3,99	3,96	3,99	3,99	3,99	3,99	3,98	3,89	3,99	3,99
Fe	0,03	0,02	0,02	0,02	0,05	0,03	0,05	0,02	0,04	0,03	0,02	0,05	0,06	0,03	0,03
Ca	0,09	0,09	0,09	0,10	0,10	0,10	0,10	0,09	0,10	0,09	0,08	0,10	0,10	0,09	0,11
Na	0,86	0,87	0,86	0,87	0,76	0,80	0,78	0,86	0,85	0,85	0,82	0,82	0,76	0,85	0,82
K	0,04	0,05	0,05	0,04	0,08	0,07	0,08	0,05	0,05	0,06	0,11	0,06	0,04	0,03	0,06
Total	5,01	5,02	5,01	5,02	5,01	5,00	5,01	5,02	5,02	5,01	5,02	5,02	5,00	5,00	5,01
Or	3,65	4,91	4,60	4,08	8,62	7,57	8,05	5,05	4,66	5,55	10,88	5,80	4,23	3,51	5,61
Ab	87,39	85,71	86,11	86,44	81,16	82,25	81,19	85,85	85,62	84,98	80,92	83,77	84,78	86,83	83,70
An	8,96	9,38	9,30	9,48	10,23	10,18	10,77	9,10	9,73	9,47	8,20	10,43	10,98	9,66	10,68

Tabela 5.4 Dados químicos obtidos a partir das análises de cristais de plagioclásio presentes no meteorito Campos Sales. Dados da fórmula estrutural obtidos a partir do cálculo para 5 átomos de oxigênio. Or= Ortoclásio, Ab= Albita, An= Anortita. C = centro, b = borda

Cristal	89	90	92	93	101	103	104	114	14	16	17	18	13
Posição	c	c	c	c	c	c	c	c	c	c	c	c	c
SiO <sub>2</sub>	64,99	65,18	65,02	65,02	65,67	65,41	64,24	65,51	64,77	65,1	65,14	64,73	64,72
TiO <sub>2</sub>									0,02	0,01		0,12	0,09
Al <sub>2</sub> O <sub>3</sub>	21,25	21,31	21,01	21,23	21,21	20,83	19,05	21,19	18,86	19,52	21,07	19,83	19,57
FeO	0,77	0,7	1	0,9	0,49	0,58	2,27	0,52	0,72	1,11	0,58	0,78	1,6
CaO	2,17	2,14	2,08	1,96	2,2	2,34	1,83	1,96	4,11	2,66	2,15	3,46	2,02
Na <sub>2</sub> O	9,75	9,84	9,88	9,9	9,68	9,81	9,26	9,98	8,66	8,99	9,63	8,98	9,12
K <sub>2</sub> O	1,07	0,83	1,01	0,99	0,75	1,02	0,95	0,84	1,02	1,09	1,28	1,07	0,79
Total	100	100	100	100	100	99,99	97,6	100	99,73	99,88	100,01	100,01	99,64
Si	2,88	2,88	2,88	2,88	2,90	2,89	2,93	2,89	2,89	2,89	2,88	2,88	2,88
Al	1,11	1,11	1,10	1,11	1,10	1,09	1,02	1,10	0,99	1,02	1,10	1,04	1,03
	3,99	3,99	3,98	3,99	4,00	3,98	3,95	3,99	3,88	3,92	3,98	3,92	3,91
Fe	0,03	0,03	0,04	0,03	0,02	0,02	0,09	0,02	0,03	0,04	0,02	0,03	0,06
Ca	0,10	0,10	0,10	0,09	0,10	0,11	0,09	0,09	0,20	0,13	0,10	0,16	0,10
Na	0,84	0,84	0,85	0,85	0,83	0,84	0,82	0,85	0,75	0,77	0,83	0,77	0,79
K	0,06	0,05	0,06	0,06	0,04	0,06	0,06	0,05	0,06	0,06	0,07	0,06	0,04
Total	5,02	5,01	5,02	5,02	4,99	5,01	5,00	5,01	5,02	5,01	5,02	5,02	5,02
Or	6,04	4,72	5,68	5,60	4,33	5,70	5,74	4,76	5,78	6,42	7,22	6,07	4,83
Ab	83,67	85,06	84,49	85,09	84,99	83,32	84,98	85,92	74,64	80,43	82,59	77,44	84,79
An	10,29	10,22	9,83	9,31	10,67	10,98	9,28	9,32	19,58	13,15	10,19	16,49	10,38

Tabela 5.5 Dados químicos obtidos a partir das análises de cristais de espinélio presentes no meteorito Campos Sales. Dados da fórmula estrutural obtidos a partir do cálculo para 4 átomos de oxigênio. C = centro, b = borda

Cristal	57	58	59	60	61	62	63	64	65	66	67	68	45	41	42	43	44	52
Posição	c	c	c	c	c	c	c	c	c	c	c	c	c	c	c	c	c	c
TiO <sub>2</sub>	2,53	2,43	2,4	2,3	2,39	2,38	2,27	2,49	2,34	2,66	1,88	2,45	2,44	2,66	2,4	2,62	2,28	2,47
Al <sub>2</sub> O <sub>3</sub>	7,1	7,09	6,61	6,41	7,49	7,14	7,03	6,67	6,41	6,36	6,47	6,55	5,61	6,41	5,86	6,38	6,33	2,89
Cr <sub>2</sub> O <sub>3</sub>	54,96	55,78	55,79	55,66	55,05	55,41	54,99	55,78	55,58	54,59	46,24	53,31	55,56	54,61	55,77	55,09	55,86	59,91
FeO	30,75	30,74	30,9	31,34	30,58	30,78	30,95	30,95	31,01	32,43	29,85	31,37	29,73	31,13	30,89	30,99	30,86	30,17
MnO	0,52	0,4	0,56	0,49	0,23	0,38	0,54	0,27	0,64				0,28	0,59	0,47	0,33	0,21	0,54
MgO	2,62	2,73	2,36	2,24	2,75	2,47	2,2	2,35	2,41	2,59	7,27	3,64	3,72	2,52	2,6	2,59	2,37	1,01
Total	98,48	99,17	98,62	98,44	98,49	98,56	97,98	98,51	98,39	98,63	91,71	97,32	97,47	98,48	98,44	98,56	98,65	97,35
Ti	0,068	0,065	0,065	0,062	0,064	0,064	0,062	0,067	0,064	0,072	0,054	0,067	0,067	0,072	0,065	0,071	0,062	0,069
Al	0,300	0,297	0,280	0,273	0,315	0,301	0,299	0,283	0,273	0,270	0,291	0,280	0,240	0,273	0,250	0,271	0,269	0,127
Cr	1,557	1,569	1,585	1,589	1,555	1,569	1,571	1,585	1,586	1,556	1,394	1,531	1,594	1,559	1,595	1,569	1,592	1,765
Fe <sup>++</sup>	0,922	0,914	0,929	0,946	0,913	0,922	0,935	0,930	0,936	0,978	0,952	0,953	0,902	0,940	0,935	0,934	0,930	0,940
Mn	0,016	0,012	0,017	0,015	0,007	0,012	0,017	0,008	0,020					0,018	0,014	0,010	0,006	0,017
Mg	0,140	0,145	0,126	0,121	0,146	0,132	0,119	0,126	0,130	0,139	0,413	0,197	0,201	0,136	0,140	0,139	0,127	0,056
Total	3,003	3,002	3,002	3,007	3,001	3,000	3,003	2,999	3,007	3,015	3,104	3,028	3,016	3,012	3,012	3,009	3,008	2,985

Tabela 5.5 Dados químicos obtidos a partir das análises de cristais de espinélio presentes no meteorito Campos Sales. Dados da fórmula estrutural obtidos a partir do cálculo para 4 átomos de oxigênio. C = centro, b = borda

Cristal	26	29	110	118	119	120	121	18	22
Posição	c	c	c	c	c	c	c	c	c
TiO <sub>2</sub>	2,2	2,05	2,76	2,73	2,88	2,98	2,97	2,41	2,08
Al <sub>2</sub> O <sub>3</sub>	6,61	6,47	6,2	6,27	6,27	6,04	6,21	8,38	8,58
Cr <sub>2</sub> O <sub>3</sub>	56,14	55,9	56,01	56,38	55,84	56,39	55,52	54,92	54,85
FeO	30,14	31,52	30,08	29,94	29,72	30,41	30,28	28,96	29,71
MnO	0,68	0,56	0,55	0,7	0,67	0,7	0,83	0,63	0,55
MgO	2,34	2,15	2,67	2,72	2,54	2,44	2,75	3,19	2,9
Total	98,96	98,65	98,35	98,8	98,55	98,96	98,66	98,91	98,91
Ti	0,059	0,056	0,075	0,073	0,078	0,080	0,080	0,064	0,055
Al	0,280	0,275	0,263	0,264	0,266	0,255	0,263	0,348	0,357
Cr	1,593	1,595	1,593	1,595	1,586	1,597	1,575	1,532	1,533
Fe <sup>++</sup>	0,904	0,951	0,905	0,896	0,893	0,911	0,908	0,854	0,878
Mn	0,021	0,017	0,017	0,021	0,020	0,021	0,025	0,019	0,016
Mg	0,125	0,116	0,143	0,145	0,136	0,130	0,147	0,168	0,153
Total	3,005	3,009	2,997	2,997	2,996	2,994	3,001	2,996	3,000

Tabela 5.6 Dados químicos obtidos a partir das análises de cristais de cloroapatita presentes no meteorito Campos Sales. C = centro, b = borda

Cristal	110	111	113	114	115	116	117	118	119	120	121	122	123	124	83	85	107	109	110
Posição	c	b	c	c	c	c	c	b	c	c	c	c	c	b	c	b	c	c	c
Na <sub>2</sub> O	0,67	0,51	0,53	0,45	0,51	0,66	0,42	0,71	0,48	0,59	0,54	0,62	0,64	0,92	0,41	0,57	0,77	0,29	0,33
MgO	0,13	0,39	0,12	0,14	0,04	0,11	0,26	0,09	0,23	0,06	0,04	0,1	0,2	0,11	0,18	0,34	0,54	0,2	0,19
SiO <sub>2</sub>	0,62	0,81	0,61	0,53	0,73	0,72	0,7	0,84	0,74	0,6	0,67	0,97	0,85	1,16	0,31	0,46	1,16	0,47	0,74
P <sub>2</sub> O <sub>5</sub>	40,41	38,07	40,06	36,3	37,76	39,04	39,06	39,83	37,31	40,56	37,76	37,2	34,49	37,17	36,7	36,97	36,58	37,24	30,99
CaO	50,64	47,68	50,55	46,36	46,55	49,76	49,37	47,53	46,39	50,5	48,17	46,63	42,03	46,12	51,43	46,76	46,65	50,25	57,45
Cl	5	4,8	5,16	4,67	4,69	4,94	4,95	5,1	4,52	5,12	4,68	4,58	4,37	4,56	4,74	4,78	4,69	4,96	4,18
F	1,11	0,81	0,43	0,65	0,76	0,63	0,45	1,47	0,49	1,07	0,08	0,77	1,95	0,62	1	0,75	1,07	0,58	0,27
CO <sub>2</sub>		1,35		9,32	5,51	2,04	2,76	2,8	5,44		3,52	5,32	11,73	5,34		6,86	2,5	0,94	
Al <sub>2</sub> O <sub>3</sub>	0,23	0,71	0,17	0,21	0,27	0,13	0,12	0,55	0,16	0,22	0,27	0,85	0,93	0,61	4,55	1,98	4,89	4,38	5,08
TiO <sub>2</sub>	0,13		0,04	0,06		0,05				0,02	0,07	0,02	0,07	0,07	0,17		0,03	0,01	
MnO	0,1		0,14	0,07		0,1	0,04		0,2	0,04	0,04	0,09	0,08	0,06	0,07	0,02	0,04	0,15	
FeO	0,44	4,22	1,49	0,85	2,53	1,11	1,34	0,54	3,64	0,76	3,65	2,47	2,18	2,73	0,4	0,45	1,01	0,45	0,69
Total	99,48	99,35	99,3	99,61	99,35	99,24	99,52	99,46	99,6	99,54	99,49	99,62	99,52	99,47	99,96	99,94	99,93	99,92	99,92

Tabela 5.7 Dados químicos obtidos a partir das análises de cristais de troilita presentes no meteorito Campos Sales. C = centro, b = borda

Cristal	19	20	21	22	23	24	1	2	117	39	40	22	23	24	25	26	42	43	44	45
Posição	c	c	c	c	c	b	c	b	c	c	c	c	c	c	c	c	c	c	c	b
S	37,64	37,41	37,91	37,84	37,62	38,23	36,52	32,84	36,63	36,78	37,49	37,57	32,43	35,2	37,08	35,16	36,23	36,9	37,13	37,21
Ti							0,01					0,1	0,07	0,06	0,11					0,03
V	0,07	0,04	0,01		0,03	0,1	0,09	0,01	0,03											0,09
Cr	0,09	0,02		0,04				0,04			0,16		0,16			0,03				
Mn	0,07	0,08		0,03	0,17		0,18	0,03	0,04			0,07		0,02		0,03	0,11	0,03		
Fe	61,81	61,55	61,72	62,06	60,51	61	60,13	62,84	61,22	59,56	59,04	58,48	65,31	60,37	59,36	57,99	59,18	53,89	60,08	60,09
Co		0,11	0,02		0,15	0,26		0,03		0,1	0,07									
Ni	0,17	0,24	0,06	0,03	1,16	0,27	0,04	0,02	0,25		0,08	0,02			0,09	0,14		1,58		
Cu		0,18				0,23			0,06	0,04	0,04									
Zn	0,15	0,36			0,14	0,22	0,01		0,14											
Si			0,28		0,36		0,35	0,46		0,24	0,25	0,34	0,25	0,41	0,52	1,22	0,23	0,69	0,3	0,26
O						2,23	2,83	1,74	2,8	2,65	2,98	1,51	3,28	2,29	4,57	2,22	6,34	2,14	2,01	
Total	100	99,99	100	100	100	100	100	99,11	99,97	99,66	99,78	99,56	99,73	99,34	99,45	99,11	97,89	99,51	99,71	99,66

Tabela 5.7 Dados químicos obtidos a partir das análises de cristais de troilita presentes no meteorito Campos Sales. C = centro, b = borda

Cristal	19	20	21	22	23	24	25	26	27	28	66	67	68	71	72	73	74	76
Posição	c	c	c	c	c	c	c	c	b	c	c	c	c	c	c	c	c	b
S	38,54	38,42	38,35	37,22	38,5	37,85	39,1	36,81	38,24	38,56	35,28	31,69	38,73	38,05	38,34	38,76	38,95	34,84
Ti		0,12	0,04		0,05	0,06	0,07	0,04		0,06	0,75	0,79	0,04					0,04
V		0,02	0,08	0,05			0,1	0,06		0,03								
Cr	0,09	0,04		0,07	0,14	0,05				0,06	0,15	0,13	0,06	0,08				0,16 0,04
Mn			0,05	0,13	0,04			0,13		0,03		0	0	0,02		0,01	0,1	
Fe	60,6	60,21	60,72	61,34	60,62	61,36	60,02	62,2	60,95	57,86	57,45	60,2	60,69	61,49	60,92	60,5	60,28	61,89
Co	0,54	0,4	0,32	0,4	0,1	0,09	0,3	0,23	0,38	0,17	0,09							
Ni	0,2	0,29	0,19	0,36	0,22	0,48	0	0,2	0,12		0,07	0,34			0,14	0,04	0,02	
Cu	0,03	0,01	0,14	0,06		0,12	0,14	0,03	0,04	0,28	0,35							
Zn		0,23	0,11							0,1								
Si		0,26		0,34	0,33		0,27	0,3	0,27	0,27	0,48	0,76	0,27	0,26	0,29	0,3	0,27	0,36
O										2,7	4,4	4,77						2,51
Total	100	100	100	99,97	100	100,01	100	100	100	100,02	99,12	98,68	99,79	99,9	99,69	99,61	99,82	99,64

Tabela 5.8 Dados químicos obtidos a partir das análises de cristais de liga metálica Fe-Ni presentes no meteorito Campos Sales. C = centro, b = borda

Cristal	44	13	14	15	16	17	18	19	20	21	22	23	24	25	26	27	28	29	32	75	76
Posição	b	c	c	c	c	c	c	c	c	c	c	c	c	c	c	c	c	c	c	c	c
Fe	79,85	81,34	81,83	82,48	81,69	80,09	80,74	82,48	82,12	81,64	82,19	81,28	82,74	80,95	85,14	81,11	79,15	80,32	85,15	82,35	84,18
Ni	16,6	14,26	14,52	14,73	14,16	16,38	14,12	14,33	14,71	13,93	14,18	13,76	13,85	14,89	11,53	15,72	16,76	16,45	10,97	15,49	13,31
Al	0,67	0,8	0,46	0,3	0,57	0,41	1,57	0,46	0,35	0,75	0,54	0,83	0,38	0,62	0,52	0,52	0,42	0,37	0,63	0,44	0,5
Co		0,86	0,96	0,52	0,49	0,65	0,77	0,65	0,73	0,74	0,82	0,75	0,55	0,68	0,68	0,82	0,83	0,96	0,81	1,27	1,13
Si	0,29	0,35	0,35	0,4	0,37	0,38		0,25	0,43	0,31	0,42	0,43	0,42	0,39			0,4	0,38	0,24		
Cu		0,06		0,1	0,13	0,26	0,3	0,16	0,13	0,2	0,11	0,17	0,17	0,13	0,08	0,19	0,4	0,2	0,07	0,01	0,08
Sc																					
Mn	0,05	0,14		0,01	0,04	0,04	0,15		0,06	0,11	0,01	0,07	0,12	0,14	0,11	0,04	0,1		0,02		0,04
Cr	0,06	0,02	0,03	0,08	0,11	0,09		0,11		0,08	0,09	0,18	0,19	0,02	0,03	0,02	0,01		0,1	0,05	0,03
Zn		0,1	0,07		0,14					0,02			0,06		0,08		0,12	0,07			0,02
V		0,08	0,05	0,04				0,03		0,01		0,08		0,02					0,02	0,05	
Ti	0,02		0,09		0,07	0,07	0,11			0,02	0,05	0,05	0,06					0,06	0,03		0,05
Total	97,54	98,01	98,36	98,66	97,7	98,37	97,72	98,55	98,56	97,78	98,39	97,52	98,61	97,88	98,19	98,42	98,19	98,81	98,02	99,63	99,39

Tabela 5.8 Dados químicos obtidos a partir das análises de cristais de liga metálica Fe-Ni presentes no meteorito Campos Sales. C = centro, b = borda

Cristal	77	78	88	104	90	87	116	38	29	30	31	29	30	31	32	33	34	35	36	37	38	
Posição	c	b	c	c	b	c	c	c	c	c	c	c	c	c	c	c	c	c	c	c	c	
Fe	83,87	81,14	84,14	86,67	78,84	81,58	66,22	62,56	45,94	46,07	46,53	58,31	61,57	61,68	63,56	64,52	64,87	64,76	64,36	64,47	61,82	
Ni	13,24	16,15	13,56	12,55	18,31	16,75	29	34,24	52,42	52,61	52,68	37,23	36,89	35,09	34,53	34,13	33,8	33,57	33,33	33,77	36,78	
Al	0,39	0,58	0,52	0,36	0,43	0,39	0,96	0,29	0,45	0,78	0,34	0,64	0,54	0,64	0,67	0,41		0,66	0,58	0,49	0,28	
Co	0,99	1,1	1,22		1,08		0,21	0,29	0,04		0,37	0,7	0,55	0,66	0,33	0,62	0,58	0,45	0,54	0,57		
Si				0,03	0,31	0,48	0,32	0,18	0,31	0,33	0,3	0,32		0,29	0,31	0,34		0,37	0,39	0,34		
Cu		0,06			0,19		0,33	0,41	0,4		0,25	0,07	0,05	0,21	0,08	0,26	0,15	0,31	0,23	0,22		
Sc										0,02												
Mn				0,07		0,05	0,08		0,07	0,13		0,05		0,07		0,15	0,02					
Cr	0,04	0,04	0,14	0,05		0,07	0,05	0,01	0,05			0,02		0,01		0	0,11	0,05	0,01	0,03		
Zn		0,07									0,02				0,03	0,16		0,39	0,03			
V	0,15		0,01			0,09					0,02	0,01		0,05	0,02	0,11	0,01		0,04			
Ti		0,19	0,05	0,07						0,06	0,06	0,08	0,06	0,03								
Total	98,68	99,33	99,64	99,8	99,16	99,32	97,26	97,98	99,7	99,98	99,91	97,31	99,84	98,41	99,99	100,01	99,95	99,78	99,8	99,99	100,01	